Review

Label-Free Impedance Biosensors: Opportunities and Challenges

Jonathan S. Daniels,[a,b] *Nader Pourmand*[a]*

[a] Stanford Genome Technology Center; 855 S. California Ave., Palo Alto, CA 94304, USA
*e-mail: pourmand@stanford.edu
[b] Stanford Center for Integrated Systems; 420 Via Palou, Stanford, CA 94305, USA

Received: December 22, 2006
Accepted: March 20, 2007

Abstract
Impedance biosensors are a class of electrical biosensors that show promise for point-of-care and other applications due to low cost, ease of miniaturization, and label-free operation. Unlabeled DNA and protein targets can be detected by monitoring changes in surface impedance when a target molecule binds to an immobilized probe. The affinity capture step leads to challenges shared by all label-free affinity biosensors; these challenges are discussed along with others unique to impedance readout. Various possible mechanisms for impedance change upon target binding are discussed. We critically summarize accomplishments of past label-free impedance biosensors and identify areas for future research.

Keywords: Impedance biosensor, Affinity biosensor, Electrochemical impedance spectroscopy, Label-free, Immunosensor

DOI: 10.1002/elan.200603855

1. Introduction

A *biosensor* is a device designed to detect or quantify a biochemical molecule such as a particular DNA sequence or particular protein. Many biosensors are *affinity-based*, meaning they use an immobilized capture *probe* that binds the molecule being sensed – the *target* or *analyte* – selectively, thus transferring the challenge of detecting a target in solution into detecting a change at a localized surface. This change can then be measured in a variety of ways. *Electrical biosensors* rely solely on the measurement of currents and/or voltages to detect binding [1–3]. Thus, this category excludes sensors which require light (e.g., surface plasmon resonance or fluorescence), use mechanical motion (e.g., quartz crystal microbalance or resonant cantilever), use magnetic particles, etc. Due to their low cost, low power, and ease of miniaturization, electrical biosensors hold great promise for applications where minimizing size and cost is crucial, such as point-of-care diagnostics and biowarfare agent detection.

Electrical biosensors can be further subdivided according to how the electrical measurement is made, including voltammetric, amperometric/coulometric, and impedance sensors. Voltammetry and amperometry involve measuring the current at an electrode as a function of applied electrode-solution voltage; these approaches are DC or pseudo-DC and intentionally change the electrode conditions. In contrast, *impedance biosensors* measure the electrical impedance of an interface in AC steady state with constant DC bias conditions. As discussed below, most often this is accomplished by imposing a small sinusoidal voltage at a particular frequency and measuring the resulting current; the process can be repeated at different frequencies. The current-voltage ratio gives the impedance. This approach, known as *electrochemical impedance spectroscopy (EIS)*, has been used to study a variety of electrochemical phenomena over a wide frequency range [4]. If the impedance of the electrode-solution interface changes when the target analyte is captured by the probe, EIS can be used to detect that impedance change. Alternatively, the impedance or capacitance of the interface may be measured at a single frequency. Impedance measurement does not require special reagents and is amenable to label-free operation as will be explained in Section 2. For the purposes of this review article, we define affinity impedance biosensors as techniques for the detection of biological molecules by measuring impedance changes of the capture probe layer.

A closely related but separate class of biosensors operates by field-effect modulation of carriers in a semiconductor due to nearby charged particles [5]. Ion-sensitive field-effect transistors (ISFETs) and relatives (EnFETs, BioFETs, etc.) are the canonical examples [6], but similar mechanisms operate in semiconducting nanowires [7], semiconducting carbon nanotubes [8], electrolyte-insulator-semiconductor structures [9–12], suspended gate thin film transistors [13], and light-addressable potentiometric sensors [14, 15]. These field-effect sensors rely on the interaction of external charges with carriers in a nearby semiconductor and thus exhibit enhanced sensitivity at low ionic strength where counterion shielding is reduced; this is explained in a recent review [16] and evidenced by the low salt concentrations often used (e.g., [7, 10]). Even though the response of field-effect sensors can be characterized by channel conductance or capacitance of the electrolyte-insulator-semiconductor

interface, we restrict this review to cases in which the impedance of the biological layer itself is measured. Note that some sensors labeled capacitive biosensors (e.g., [17–20]) are measurements of probe-insulator-semiconductor interfaces where capacitive changes might occur both within the semiconductor (due to the field effect) and also within the probe layer (the focus of this review). Deconvolving the contributions is difficult, and these sensors will be largely excluded from this review.

Impedance biosensors can detect a variety of target analytes by simply varying the probe used. Here we focus on detection of DNA and proteins. Among impedance sensor applications not discussed here are small molecule sensors (e.g., [21–24]), cell-based biosensors (e.g., [25–28]), and lipid bilayer sensors (e.g., [29, 30]).

This review article focuses on general principles of label-free affinity impedance biosensors and compares the methods and results of different investigators. For further reading, we refer the reader to an excellent 2003 review of impedance biosensors by Katz and Willner that focuses on faradaic techniques and impedance amplification using labels [31]. An earlier review of capacitive biosensors includes capacitive biosensors on semiconductor substrates with field-effect contributions [32]. Classic texts by Macdonald on EIS [4] and Bard/Faulkner on electrochemistry [33] are good resources. Various approaches to electrical protein sensors were reviewed in 1991 and 2000, but only touch cursorily on impedance methods [34, 35]. Various electrochemical DNA detection approaches were reviewed by Gooding [36] and more recently by Moeller [37], similarly treating impedance techniques only briefly. Thévenot recommended definitions and elucidated relevant performance criteria for the entire field of electrical biosensors [1].

In Section 2 we discuss the motivation for studying impedance biosensors in general, and label-free systems in particular. Important affinity biosensor concepts are discussed next, focusing on limits to biosensor performance. Details relating to the impedance measurement are explained in Section 4, and subsequently we discuss the possible mechanisms of binding-modulated impedance and briefly summarize other practical details. In Section 6 we critically review prior research on affinity impedance biosensors, focusing on label-free DNA and protein sensors, through the end of 2006. To conclude, we summarize the status of affinity-based impedance biosensors and identify the challenges inhibiting increased application and commercialization. We attempt to paint a balanced picture between the progress being made and oft-minimized obstacles in this still-nascent research area.

2. Why Study Impedance Biosensors?

The most promising applications of electrical biosensors are situations where low cost, small instrument size, and speed of analysis are crucial, but cutting-edge accuracy and detection limits are not. *Point-of-care diagnostics* – a measurement and diagnosis at a bedside, in an ambulance, or during a clinic visit – are a promising application [38–40]. If the cost and time per data point were reduced, screening for various cancer and disease markers using an electrical biosensor could become part of routine medical checkups. Other applications include biowarfare agent detection, consumer test kits, bioprocess monitoring, and water quality testing. One key question is whether impedance biosensors can have sufficient selectivity for use in real-world applications, because actual samples typically contain an uncontrolled but significant amount of nontarget molecules. Another potential application is the label-free determination of biomolecular affinity coefficients, in which pure target samples are used. In short, impedance biosensors have potential for simple, rapid, label-free, low-cost detection of biomolecules.

2.1. To Label or Not to Label?

Arguably the major motivation for studying impedance biosensors is their ability to perform label-free detection. Most biosensors require a *label* attached to the target; during readout the amount of label is detected and assumed to correspond to the number of bound targets. Labels can be fluorophores, magnetic beads, active enzymes with an easily detectable product, or anything else allowing facile target conjugation and convenient detection. However, labeling a biomolecule can drastically change its binding properties, and the yield of the target-label coupling reaction is highly variable [41]. These issues are relatively minor concerns for DNA sensors, but are especially problematic for protein targets.

Thus, an indirect labeling scheme often referred to as a sandwich assay is commonly used for protein detection (see Fig. 2) [42, 43]. This requires two probes that bind to different regions of the target, yielding enhanced selectivity but increasing development costs and limiting use in research settings. The first probe is immobilized on the solid support, the analyte is introduced, and then a secondary probe is introduced after washing. This second probe is labeled or can be detected by introducing yet another labeled probe that binds to all the secondary probes. The widespread ELISA (Enzyme-Linked ImmunoSorbent Assay) technique is the canonical example of a sandwich assay [44].

2.2. Label-Free Operation

When a target biomolecule interacts with a probe-functionalized surface, changes in the electrical properties of the surface (e.g., dielectric constant, resistance) can result solely from the presence of the target molecule. Thus, no label is required for impedance sensing; this is particularly advantageous for protein detection as explained above. However, because labeling can augment selectivity (e.g., using the sandwich approach with second probe) and enhance sensi-

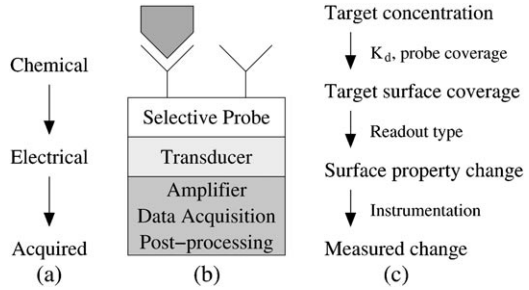

Fig. 1. Generalized affinity biosensor, showing a) the signal flow, b) the physical arrangement, and c) the steps involved.

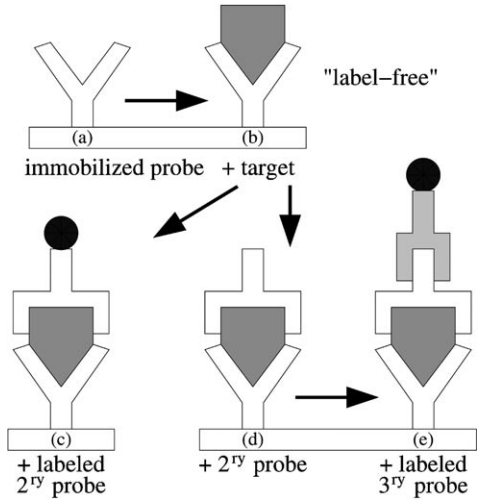

Fig. 2. Generalized sandwich assay. The secondary antibody can provide increased selectivity and allows a well-known entity to be labeled instead of the (variable) target. However, a label-free scheme allows real-time detection and eliminates the time and cost of labeling.

tivity (e.g., using a label that greatly changes the impedance), some impedance biosensors in the literature use a label. However, labeling requires extra time, expense, and sample handling. In this review we treat only label-free sensors.

Besides the time and expense benefits of omitting the labeling step, label-free operation enables detection of target-probe binding in real time [45], which is generally not possible with label-based systems. Real-time sensing confers at least two major advantages over endpoint detection. First, time averaging of binding/unbinding events can improve measurement accuracy. Second, it allows determination of affinity constants by curve-fitting the sensor output vs. time [46]. For accurate results, effects including diffusion rate and steric hinderance must be accounted for, just as in SPR [47]. Furthermore, it is important to know the relationship between the amount of bound target and sensor output signal (see Sec. 5.2).

Quartz crystal microbalance (QCM) [48], related mechanical techniques [49], and SPR [47, 50] are notable examples of nonelectrical, label-free, real-time biosensors (overview in [51]). One challenge with any type of label-free biosensors is that a relatively small change in surface properties occurs upon binding, requiring sensitive readout methods. Selectivity in complex samples poses another major challenge, as discussed in Section 3.3.

3. Affinity Biosensor Concepts

3.1. Affinity Biosensor = Affinity + Sensor

As depicted in Figure 1 and represented in the term itself, affinity-based biosensors divide the problem of detecting a particular biomolecule into two parts: (1) binding the desired target while excluding nontarget binding (we call this the *affinity step*) and (2) detecting a change in the surface properties (the *readout step*). The affinity step is based on the surface chemistry and biological binding, while the readout step is based on the physics of detection plus all associated signal processing. Though these steps can be studied and optimized independently, they are intertwined in the final system, and either can limit overall performance.

3.2. Probe-Target Binding

Affinity biosensors are based on a probe binding a target and can thus be treated in terms of receptor-ligand binding theory [42, 52, 53]. The fraction of probe bound at equilibrium (θ) is determined by the relative values of the dissociation constant K_d and target concentration:

$$\theta = \frac{[\text{Probe} \cdot \text{Target}]}{[\text{Probe}] + [\text{Probe} \cdot \text{Target}]} = \frac{[\text{Target}]}{[\text{Target}] + K_d} \quad (1)$$

This is one form of the Langmuir adsorption isotherm, which describes surface binding for identical noninteracting binding sites. Increasing the surface probe density σ leaves θ unchanged but allows the measured surface property change – typically related to the actual density of target molecules bound, or $\sigma\theta$ – to increase. However, too high of a probe density may actually inhibit target binding due to steric hinderance or other effects [54, 55].

Despite the ability to monitor binding in real-time, the majority of published label-free impedance biosensors make a measurement only after equilibrium has been reached. However, kinetic considerations are particularly important (1) at low concentrations, where detection limits are usually determined [56, 57] and (2) when target diffusion to the probe surface takes longer than the binding interaction [58].

3.3. Selectivity

Affinity-based biosensors exploit the selectivity of the probe to confer selectivity to the overall sensor. *Selectivity*, sometimes termed specificity despite contrary recommendations

[59], means that the sensor responds only to the target analyte and not to other similar molecules. Generally speaking, label-free biosensors cannot distinguish between specific and nonspecific interactions except by probe selectivity, regardless of the readout method.

Selectivity is especially important in real-world samples where the target concentration can be much less than the concentration of nontarget biomolecules present. For instance, blood serum typically contains ca. 70 mg/mL total protein content, yet prostate specific antigen (PSA), a biomarker for prostate cancer, needs to be detected at ca. 2 ng/mL [60, 61]. Thus, a biosensor that can detect 1 ng/mL PSA in saline but manifests even a 1 ppm response to blood proteins would be useless in a clinical setting unless the serum is depleted of interfering proteins or some other compensation is made. Thus, a trade-off exists between selectivity requirements and sample preparation complexity for most real-world applications. It is the opinion of the authors that obtaining adequate selectivity in complex real-world samples is the most daunting challenge to the field of biosensors in general, including impedance biosensors.

A closely related concept is *nonspecific binding*, in which nontarget biomolecules stick to the probe layer, preventing target binding or causing a false positive signal. To alleviate this problem, the sensor chamber is often preexposed to a solution containing a *blocking agent* such as bovine serum albumin (BSA) or salmon sperm DNA which nonspecifically adsorbs (hopefully not occupying the probe binding sites), reducing subsequent nonspecific binding from the actual sample. *Antifouling agents* such as polyethylene glycol can also be deposited on areas surrounding the sensor to prevent target depletion via nonspecific binding [62 – 64]. Use of blocking agents is not a systematic science, but several approaches have been found to work in specific situations (e.g., [65 – 67]). A differential sensor scheme can be used to (imperfectly) subtract out the nonspecific component of the sensor response (see Sec. 5.3). Washing the sensor surface before readout can sometimes improve selectivity by washing away nonspecifically adsorbed molecules while leaving the target intact, but this in an endpoint measurement and not real-time approach. In a *homogeneous assay* this washing step is not necessary [68].

3.4. Limit of Detection and Reproducibility

The most cited figure of merit for any chemical sensor is the *limit of detection*, or the smallest amount of target that can be reliably detected. Occasionally the term *sensitivity* is used, which can also refer to the slope of the response curve [69, 70]. Unfortunately, there is no universal method for determining the limit of detection, complicating comparison of published results. The detection limit can be determined by measuring the sensor response to a dilution series and determining the target smallest concentration at which the sensor response is clearly distinguishable from the response to a blank solution. However, some investigators do not measure the sensor response to a blank solution (not necessarily zero) and thus may state an overly-optimistic detection limit. Other investigators calculate a limit of detection based on the slope of the dose-response curve and the standard deviation of the blank response according to [71], without actually demonstrating reproducible detection at the reported concentration.

Detection limits are almost always determined in the absence of confounding nontarget biomolecules. Because such clean samples rarely occur in real-world applications, reported limits of detection are not necessarily a good predictor of real-world performance. To demonstrate clinical utility, biosensors should be challenged with mixed target/nontarget samples to simultaneously test selectivity and sensitivity.

Fundamentally, the achievable limit of detection is bounded by the strength of the probe-target interaction (see (1) or [74]) together with the minimum detectable $\sigma\theta$; for this reason commercial ELISA kits with identical readout technology have varying limits of detection for different targets. Real-time readout may improve the achievable detection limit by monitoring the transient sensor response, allowing the binding signal to be separated from the slower nonspecific adsorption signal and drift in the readout electronics.

Variation between sensors impacts the practical detection limit because a separate calibration step rarely can be performed for each sensor. Many investigators do not account for such variation when reporting detection limits because of the large number of experiments required. However, reproducibility will affect the limit of detection for any real-world application.

Because of the two-step detection scheme, the limit of detection in many practical situations is dictated by nonspecific binding and/or lack of sensor reproducibility. However, for impedance biosensors, the reported detection limit is often the target concentration required to induce the minimally-detectable change in impedance based on the intrinsic electronic noise of the impedance readout.

Requirements for the limit of detection vary widely by application. As examples, consider that the aforementioned cancer biomarker PSA needs to be detected at ca. 2 ng/mL [60, 61]. Human chorionic gonadotropin, used in home pregnancy tests and also as a cancer marker, indicates pregnancy when above 5 ng/mL in urine but exceeds 1 μg/mL several weeks into pregnancy [72, 73]. Other biomarkers of clinical interest, such as cytokines, exist in the blood in pg/mL concentrations. Conventional techniques like ELISAs routinely obtain pg/mL detection limits if the probe-target affinity is high.

3.5. Dynamic Range

If the sensor is to be used to quantify the analyte concentration and not just detect its presence, the range of measurable concentrations is important. The *dynamic range* is the ratio of the largest measurable target concentration and the limit of detection. The upper limit is almost invariably

set by the saturation of the probe with target molecules ($\theta = 1$), and thus is determined by the affinity step. Dynamic range can be extended on the upper end by simply performing measurements with dilution series of the sample. Real-time measurements also can enhance dynamic range.

The smallest detectable change in target concentration is the *resolution* (defined as output uncertainly, due to both systematic and irreducible noise, divided by the slope of the response curve). While uncommon in the affinity biosensor literature, we propose that resolution be given more prominence in characterizing affinity biosensors when the application requires target quantification.

3.6. Amplification

All chemical amplification schemes for electrical biosensors, to the authors' knowledge, rely on either target labeling (including sandwich approach) or cycling of a redox species. Thus amplification techniques lay outside the domain of label-free impedance biosensors and are mentioned here only for completeness. One impedance amplification approach is the (enzyme) label-catalyzed precipitation of an insoluble material onto the electrode [75–78]. Electroless deposition of silver onto metallic nanoparticle labels has also been used [37, 79–81]. Various methods have been reported for post-affinity attachment of charged and/or bulky particles that alter the interface impedance [82–85].

3.7. Multiplexing

Detecting several targets in the same biological sample is possible if different surface regions are functionalized with different probes. Multiplexing is desirable because it reduces both cost and sample volume per data point. Because electrical signals are readily steered, it is possible to detect various analytes using a single readout circuit. Regardless of readout mechanism, multiplexed protein detection is complicated by cross-reactivities – a probe binds to multiple targets or vice versa – which severely limits the possible degree of multiplexing and is especially troublesome in real-world situations [86–88]. However, a panel of several biomarker measurements has far more diagnostic power than a single biomarker can provide [89]. Thus, efforts to develop multiplexed protein biosensors will surely continue, though the challenge of cross-reactivity cannot be ignored. For most label-free biosensors, including impedance biosensors, the principal limitation on multiplexing arises from the affinity step and not the readout step.

3.8. What Really Limits Biosensor Performance?

It is apparent that the limits of label-free affinity biosensor performance are more often set by the affinity step than the readout step. This suggests the need for further research efforts in probe immobilization chemistries and minimization of nonspecific binding, while recognizing the fundamental limits of finite probe affinity, selectivity, and density.

Where the affinity step limits system performance, it is crucial to realize that readout techniques with inherently worse detection limits can be used to obtain overall equal results. Some investigators claim that impedance techniques have extremely low limits of detection compared with optical or other readout methods (e.g., [32]) while others disagree (e.g., [90]). The authors are of the opinion that the readout sensitivity afforded by impedance sensing is inferior to many other techniques but is sufficient for many applications, precisely because often the affinity step bounds the overall biosensor performance. Impedance biosensors may also be useful when moderate sensitivity is required at a very low cost and/or using a very small instrument. However, the authors doubt that label-free affinity impedance biosensors will ever achieve the same sensitivity as label-based techniques such as conventional ELISAs due to the limitations of both label-free detection (eliminating the possibility of chemical amplification) and sensitivity of impedance readout.

4. Measuring Electrochemical Impedance

4.1. Apply a Voltage, Measure a Current

Electrical impedance is defined as the ratio of an incremental change in voltage to the resulting change in current. Either an AC test voltage or AC test current is imposed while the other variable is measured. Mathematically, if the applied voltage is $V_{test} = V_{DC} + V_{AC}\sin(\omega t)$ and the resulting current is $I_{test} = I_{DC} + I_{AC}\sin(\omega t - \varphi)$, then the complex-valued impedance $Z(\omega)$ has magnitude V_{AC}/I_{AC} and phase φ. The electrode-solution impedance depends on both the bias conditions (V_{DC}) and the measurement frequency (ω). By exciting with a single frequency, a lock-in amplifier can be used to accurately measure the output signal at the same frequency. Voltage excitation is usually employed in EIS because the most troublesome parasitic impedances are in parallel with the measured electrode-solution impedance. In most cases, the measurement process is repeated at different frequencies, yielding $Z(\omega)$.

In impedance biosensors, the applied voltage should be quite small – usually 10 mV amplitude or less – for several reasons. First, the current-voltage relationship is often linear only for small perturbations [91], and only in this situation is impedance strictly defined. A second reason is to avoid disturbing the probe layer; covalent bond energies are on the order of 1–3 eV but probe-target binding energies can be much less (and in some cases the probe is not covalently attached to the electrode), and applied voltages will apply a force on charged molecules. This second consideration also applies to DC bias voltages across the electrode-solution interface. Correctly performed, electrochemical impedance spectroscopy does not damage the biomolecular probe layer, an important advantage over voltammetry or amperometry where more extreme voltages are applied.

Variations of standard impedance spectroscopy include using multiple excitation frequencies simultaneously [92, 93], exciting with white noise [4], and exciting with a voltage step (which contains many frequency components) [94]. Such approaches could decrease the time required per measurement and avoid complications due to the fact that impedance is ill-defined if the system is changing during the measurement.

4.2. Electrodes

At minimum two electrodes are needed to measure electrolyte-solution impedance, and usually three are used. The current is measured at the *working electrode* and is biofunctionalized with the probe. In order to establish a desired voltage between the working electrode and solution, electrical contact must be made with the solution using a reference electrode and/or counter electrode. A *reference electrode* maintains a fixed, reproducible electrical potential between the metal contact and the solution, allowing a known voltage to be applied. A simple piece of wire – a pseudoreference or quasireference electrode [95] – can sometimes suffice. A *counter electrode* supplies current to the solution to maintain the desired electrode-solution voltage, usually in electronic feedback with the reference electrode monitoring the solution voltage.

4.3. Instrumentation

A potentiostat imposes a desired command voltage between the solution and working electrode while simultaneously measuring the current flowing between them. As described above, the command voltage for impedance sensing is an AC excitation plus an optional DC offset, and the impedance is simply the ratio of the AC voltage to the AC current. *EIS analyzers* are potentiostats designed especially for measuring AC impedance, and have typical frequency ranges of 10 MHz – 100 kHz. Computer control is ubiquitous for both potentiostats and EIS analyzers, and digital post-processing is commonly employed.

4.4. Faradaic vs. Nonfaradaic

It is important to distinguish between nonfaradaic and faradaic biosensors. In electrochemical terminology, a *faradaic* process is one where charge is transferred across an interface. However, transient currents can flow without charge transfer in *nonfaradaic* processes (e.g., charging a capacitor). In *faradaic EIS* a redox species is alternately oxidized and reduced by the transfer of an electron to and from the metal electrode. Thus, faradaic EIS requires the addition of a redox-active species and DC bias conditions such that it is not depleted. In contrast, no additional reagent is required for nonfaradaic impedance spectroscopy, rendering nonfaradaic schemes somewhat more amenable to point-of-care applications. The term *capacitive biosensor* usually designates a sensor based on a nonfaradaic scheme, usually measured at a single frequency.

4.5. Data Fitting

The measured impedance data can be used to extract equivalent values of resistances and capacitances if a circuit model is assumed a priori, though there is not a unique model or even necessarily a one-to-one correspondence between circuit elements and the underlying physical processes [96]. Figure 3 shows typical circuit models, and Figure 4 shows example impedance data. It is not always

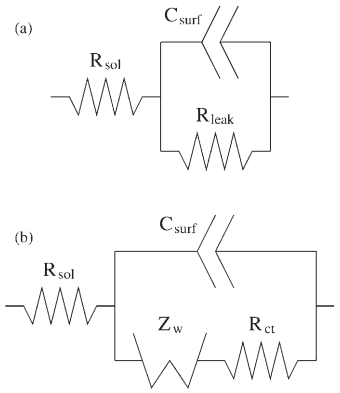

Fig. 3. Common circuit models for a) nonfaradaic and b) faradaic interfaces. See Section 4.6 for circuit elements.

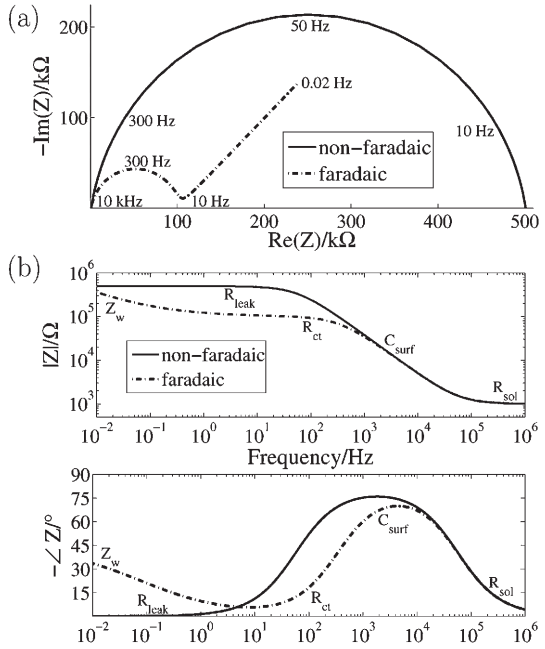

Fig. 4. Example nonfaradaic and faradaic impedance data in both Nyquist (a) and magnitude/phase (b) representations, along with dominating element. $R_{sol} = 1$ kΩ, $C_{surf} = 10$ nF with $m = 0.9$, $R_{leak} = 500$ kΩ, $R_{ct} = 100$ kΩ, and Z_w coefficient 10^{-5}.

necessary to fit the data to a model, and even the best models of the electrode-solution interface do not perfectly fit data or else require so many fitting parameters as to be useless. Sometimes the raw impedance data is fit to a model and changes in model elements are reported as the sensor output. Other times, the impedance at a particular frequency is used. Depending on the values of the respective model circuit parameters, data at a particular frequency can contain information about various circuit elements or be dictated primarily by one element, as indicated in Figure 4b.

Complex nonlinear least squares (CNLS) fitting [97] is needed to incorporate both magnitude and phase in the fitting process and is available in several free (e.g., LEVM) and commercial (e.g., ZView, ZSimpWin) software packages. Interpreting impedance spectra is sometimes more art than science, as is discussed in [98]. The *Kramers–Kronig transform* can act as an independent check against invalid experimental data [4, 96].

4.6. Circuit Models

Figure 3 shows the two most common models used to fit impedance biosensor data, depending on whether a faradaic or nonfaradaic measurement is made. The solution resistance R_{sol} arises from the finite conductance of the ions in bulk solution, and thus is generally not affected by binding. The capacitance between the metal electrode and ions in solution, C_{surf}, can be modeled as a series combination the surface modification capacitance and the double layer capacitance (see Sec. 4.8). The component due to surface modification depends on the thickness and dielectric constant of the probe layer. It can be thought of as a parallel plate capacitor, whose capacitance is given by $C = \varepsilon_r \varepsilon_0 A/t$ where ε_r is the relative dielectric constant, A is the electrode area, and t is the insulator thickness. The capacitance C_{surf} is often modeled by a *constant phase element* (see Sec. 4.7) instead of a pure capacitance.

In parallel with this capacitance there is a resistive path modeled by R_{leak} for nonfaradaic sensors or the series combination of Z_w and R_{ct} for faradaic sensors. For an ideal insulator or when no redox species is present, R_{leak} is theoretically infinite; in practice it is finite due to reasons discussed below. The *Warburg impedance* (Z_w), only of physical significance in faradaic EIS, represents the delay arising from diffusion of the electroactive species to the electrode [33, 96]. It is only appreciable at low frequencies, is affected by convection (and thus may be invalid for experimental time scales), and has a phase shift of -45°. The *charge transfer resistance* (R_{ct}) is a manifestation of two effects: (1) the energy potential associated with the oxidation or reduction event at the electrode (i.e. the overpotential) along with (2) the energy barrier of the redox species reaching the electrode due to electrostatic repulsion or steric hinderance. The two circuit elements most commonly used as indication of affinity binding are C_{surf} for nonfaradaic biosensors and R_{ct} for faradaic ones.

4.7. Constant Phase Element

It has long been recognized that the impedance of solid electrodes usually deviates from purely capacitive behavior; this is empirically modeled as a *constant phase element (CPE)*. The complex impedance of a CPE is given by $1/(j\omega A)^m$, where A is analogous to a capacitance, ω is the frequency expressed in rad/s, and $0.5 < m < 1$ ($m = 1$ corresponds to a capacitor and $m = 0.5$ corresponds to a Warburg element; m for C_{surf} modeling is typically between 0.85 and 0.98). This introduces a sub-90° phase shift, or equivalently a frequency-dependent resistor in addition to a pure capacitor.

CPE behavior has come to be expected on solid electrodes by experimentalists and can be explained mathematically by dispersion in local capacitance values. Microscopic roughness can cause this effect [99, 100], but a convincing review by Pajkossy [101] suggests that microscopic chemical inhomogeneities and ion adsorption play an even larger role (supported by data in [102–104]). Jorcin demonstrated that both surface effects and inhomogeneous current distribution contribute to CPE behavior [105]. Solid electrodes can be expected to have a certain amount of CPE behavior, and thus modeling the electrode-solution interface as purely capacitive is often simplistic and can reduce the quality of data fitting.

4.8. Double Layer Capacitance

When an electrode is polarized relative to the solution, it attracts ions of opposite charge. This tendency is countered by the randomizing thermal motion of the ions, but results in a local buildup of excess ions of opposite charge. Thus, any electric field arising at the electrode or within ionic solution decays exponentially because the excess ions screen the field. The characteristic length of this decay, or *Debye length*, is proportional to the square root of ion concentration [33] (about 1 nm for biological ionic strengths). This effect creates a capacitance called the *double layer capacitance* or *diffuse layer capacitance*.

This arrangement of a bare electrode and nearby layer of ions is conceptually similar to a double-plate capacitor, with thickness of the Debye length [106], corresponding to ca. 70 $\mu F/cm^2$ for bare metal next to solutions of biological ionic strength. Ions adsorbed to a bare electrode increase the capacitance as well, as accounted for in the Gouy-Chapman-Stern model [33]. The double layer capacitance is voltage-dependent because increasing the electrode voltage attracts the diffuse ion layer, increasing the capacitance [33]. If an insulator (e.g., an insulating probe layer) covers the electrode, forming a capacitance, the double layer capacitance appears in series with it. In impedance biosensors, the ionic double layer usually plays a minor role in the overall measured impedance by design, either because it is so large relative to series capacitance of the probe layer (for nonfaradaic sensors), or else because the parallel path through Z_w and R_{ct} dominates at relevant frequencies (for faradaic sensors).

4.9. Scaling Electrode Size

What is the optimal electrode size for affinity impedance biosensors? Electrode size greatly impacts the actual impedance measured, and can be chosen so that the instrument's frequency range yields as much useful information as possible. Conversely, the range of measurement frequencies can be chosen according to what circuit element one is trying to measure. It is unclear whether measurement at higher frequencies is desirable from the instrumentation standpoint. Higher frequencies will be less affected by drift and noise in the measurement electronics, but also complicate laboratory data acquisition and increase errors from parasitic capacitances and inductances. It is unclear from the primary literature the extent to which the biomolecules have a frequency-dependent dielectric constant (treated in Section 5.1). Several investigators report unexplained impedance drift at frequencies of roughly 100 Hz and below, while others routinely make such measurements.

Decreasing C_{surf} (e.g., by reducing the electrode area or increasing insulator thickness) increases the capacitive impedance, allowing measurement of capacitive behavior at higher frequencies. Decreasing R_{sol} (e.g., by increasing salt concentration) mainly affects the high-frequency impedance plateau, and shifts the transition region slightly to higher frequencies. For nonfaradaic sensors, decreasing R_{leak} tightens the circle in the Nyquist representation, shortens the transition region in the Bode magnitude plot, and makes it difficult to measure C_{surf} at low frequencies. If a typical nonfaradaic system is scaled down in in all dimensions by a factor $\lambda < 1$, C_{surf} and Z_w will decrease by λ^2 (increasing the impedance), R_{leak} and R_{ct} will increase by λ^2, and R_{sol} will decrease by λ. Thus, isomorphically decreasing the cell dimensions is expected to shift the impedance curve to higher frequencies and higher impedances. It also increases the range of frequencies over which C_{surf} dominates, but the transition frequency between R_{leak} and C_{surf} remains unchanged. This simple analysis neglects many second-order effects such as electrode shape and nonuniformity of current flow at the electrode.

Furthermore, decreasing the sensor area reduces the absolute number of immobilized probes. While the fractional impedance change upon target binding is expected to remain constant, the absolute change is smaller and thus may be more difficult to measure, depending on the noise or drift inherent in the measurement process.

The authors are not aware of a theoretical treatment of scaling considerations for impedance biosensors akin to the cursory analysis above; this is a serious need. Madou provided a general treatment of biosensor miniaturization and discusses scaling other varieties of electrical biosensors [107]. It has also been shown that scaling any type of affinity biosensor leads to tradeoffs between settling time and limit of detection [57, 108, 109].

5. Practical Issues in Label-free Impedance Biosensors

5.1. What Causes an Impedance Change?

What actually causes the measured impedance change in a label-free impedance biosensor? Displacement of water? Change in dielectric properties? Increased resistance to faradaic current stemming from electrostatic repulsion? Other phenomena? Various theoretical models have been proposed to explain the observed change in impedance upon target binding. An improved understanding of the connection between target binding and impedance change would enable improved biosensor design and sensitivity. Different investigators utilize different types of changes, even to detect the same target.

In general, for label-free measurements it is expected that impedance changes will be most pronounced if the target is substantially larger than the probe or has significantly different properties (dielectric constant, charge state, etc.) [32]. However, various investigators have obtained results not explained by this simple hypothesis, using nearly identical sensors with different targets (e.g., [110, 111]). Effects due to the affinity step (e.g., probe immobilization density, K_d, loss of probe activity, etc.) may or may not explain the discrepancy.

A charged surface presents either an attractive or repulsive force on ions near the electrode; this is especially applicable to faradaic sensors because the interaction of the charged redox species with the charged probe layer can significantly impact R_{ct} (the same phenomenon could also be observed by a shift in the redox potential, e.g., [112]). This effect has been used to rationalize changes in R_{ct} upon binding of a charged target for SAMs [113], for DNA sensors [114, 115], and for protein sensors [116–118]. Note that surface charge is also dependent on pH, temperature, and other factors.

Impedance might be affected in certain situations by the ability for the surface groups to be ionized. In acid-terminated SAMs, changing the pH changes the charge state of the terminal acid and can affect the measured capacitance by up to 50% [119, 120]. The impact of this effect diminishes with increasing chain length and increasing ionic strength (as expected by a series capacitance model), and involves a complex interplay between electrode potential, the repulsion or attraction of charged ions to the surface [121, 122] and possibly solvent structure [120]. Conceptually this is similar to the Stern layer of bound charge added to the Gouy-Chapman double layer model (see Sec. 4.8), and is treated theoretically in [123, 124]. Miura et al. noted a 40% increase in capacitance upon capture of K^+ at a SAM-electrolyte interface [125]. Note that the probe and target molecules usually have pH-dependent charge states (usually referred to in terms of the pI, or pH at which the net charge is zero), as can the probe attachment surface. This implies that pH needs to be carefully controlled, ideally being treated as a common-mode disturbance using a differential method (see Sec. 5.3).

For acid-terminated SAMs at pH values where the terminal acid is partially ionized, the applied voltage in EIS actually induces protonation/deprotonation, which contributes significantly to the measured impedance at frequencies near 10 Hz depending on exact kinetics of (de)protonation; this phenomena was recently treated experimentally and theoretically [126] and is a physical explanation for finite R_{leak} in nonfaradaic sensors. This suggests that surface ionization may introduce an additional impedance component that is pH-dependent and not usually modeled (a model is derived in [126]). Janek et al. also noted an anomalous impedance at low frequencies, perhaps due to this effect or due to dipole effects [127].

Applying a voltage between electrode and solution can cause the thickness of a DNA coating to either increase or decrease, presumably due to the interaction of the charged electrode with the charged DNA [128]. Changes in film thickness have also been observed in certain short peptides having an intrinsic dipole moment [129] and in loosely-packed gold-thiol SAMs [130]. Probe layer thickness in turn affects measured impedance. Likewise, an applied voltage might induce change in conformation for any probe/target pair with net charge, and is a plausible mechanism for impedance change.

Changes in molecular conformation could also introduce a change in impedance, both in C_{surf} and R_{ct}. The former was exploited for a sensor using a protein whose conformation changed upon binding of heavy metal ions [22] (though other possible explanations exist, cf. [125]). It has been shown that dsDNA conformation changes can be induced by varying ionic and/or pH conditions; this can result in significant changes in measured R_{leak} and R_{ct} [114, 131].

It has been noted that ssDNA is floppy and thus prone to lying near the surface, implying that ions might have greater access to the surface after hybridization [16, 132]. However, any steric decrease in R_{ct} upon hybridization competes with an electrostatic increase due to additional fixed charge. C_{surf} might also increase upon hybridization, as ions would be able to come closer to the electrode surface, but there are confounding effects.

In nonfaradaic sensors, it is common to rationalize changes in C_{surf} as occurring due to displacement of water and ions from the surface upon target binding. Binding should increase thickness and/or decrease ε_r of the probe layer ($\varepsilon_r \approx 2-5$ for biomolecules versus 80 for water), both decreasing capacitance. A typical conceptual explanation includes three capacitors in series: dielectric layer of the insulation (SAM or otherwise), dielectric layer of the probe layer, and the double-layer capacitance. To allow measurement of the probe layer capacitance, the insulating layer should be as thin as possible [32, 133]. Imperfect insulation, modeled by R_{leak} in parallel with the capacitance, can reduce the sensitivity of the measured impedance to the change in C_{surf}. Changes in R_{leak} are occasionally employed as a sensor output, as in [114, 134], and can be be independently assessed using cyclic voltammetry with a redox couple.

Dipoles in the SAM headgroup can contribute to measured capacitance because dipoles affect the dielectric constant ε_r [135, 136]. This observation could partially explain variation in response between otherwise similar targets. Note that ε_r is not strictly constant over frequency, as dipoles may be able to react to slow-moving excitation fields but not to higher-frequency ones. This research area, termed *dielectric spectroscopy* [137], has received limited attention in the biosensing community [138–140] but tends to be applied to measuring bulk solutions at high frequencies ($\gg 1$ MHz, C_{surf} negligible) and is thus quite distinct experimentally from conventional surface-sensitive impedance biosensors ($\ll 1$ MHz, C_{surf} important). Some biomolecule dielectric relaxation effects may be detectable at frequencies in the kHz range [138, 141]. However, these effects are usually neither surface-sensitive nor specific, so dielectric spectroscopy seems better suited to studying the behavior of biomolecules (e.g., [142]) than distinguishing between similar biomolecules. Gebbert et al. rationalized the use of kHz measurement frequencies by estimating that the dipole response of a bound antibody/antigen pair occurs at 6 kHz or below [133], though this was not experimentally determined. Measuring at frequencies corresponding to dielectric relaxation times between those of free and bound molecules might give some binding-specific information. Changes in ε_r over the range of measurement frequencies is not typically modeled during the curve fitting process; while irrelevant for most impedance biosensors, this idea provides an avenue for exploration.

Particularly in the case of polymer-immobilized impedance biosensors, the target binding event might modulate the properties of the surrounding material in such as way that the impedance changes [143, 144], akin to field effect sensors (see Sec. 1). Polymer-coated electrodes (see Sec. 6.5) often have an impedance that varies significantly with applied DC bias [145]. The double-layer capacitance (see Sec. 4.8) also depends weakly on DC bias [33, 135].

Finally, a measurable impedance change might arise from increase in DNA conductivity upon hybridization. Though not fully understood, dsDNA has significant electronic conductivity due to the base pair stacking [131, 146, 147]. While this property has been used to detect DNA hybridization using redox labels or redox-active intercalators (e.g., [148]), measuring changes in DNA conductance via impedance spectroscopy would likely be difficult to distinguish from changes in R_{sol}. The fact that DNA is a polyelectrolyte surrounded positive counterions can also affect surface impedance; DNA traps counterions, creating a local high-salt environment, implying that the ionic strength at the surface (which determines double layer capacitance) can be different than that of the bulk solution [112].

5.2. Response Curve

The response curve is the relationship between the sensor output variable (e.g., R_{ct}, change in imaginary part of the impedance at a particular frequency, etc.) and the target concentration. For all affinity biosensors, this response curve arises from two separate relations. The first corre-

sponds to the affinity step (θ([Target]), relating target surface coverage to bulk concentration), while the second corresponds to the readout step ($\Delta Z(\theta)$, relating impedance change to surface coverage). When [Target] $\gg K_d$, $\theta \approx 1$ and the impedance response saturates. For [Target] $\ll K_d$, $\theta \propto$ [Target]. Most of the reported explanations for the impedance change (see Sec. 5.1) predict $\Delta Z \propto \theta$, and thus one would expect the sensor output to be proportional to the target concentration in the low-concentration regime.

In contrast to this prediction, it is commonly observed that the response curve is logarithmic in [Target] until saturation (e.g., [133, 149, 150]) as pointed out by Bart et al. [151]. If the probe-target binding energy is heterogeneous (e.g., polyclonal antibody probes or distribution in binding site availability), then the assumptions of the Langmuir isotherm are violated and the Temkin isotherm is a better model [152]. Because the Temkin isotherm predicts $\Delta Z \propto$ log([Target]), this might explain the observed response. It is also possible that the relationship between target coverage and impedance response $\Delta Z(\theta)$ is logarithmic, as is the case with most field-effect biosensors [153]. Some authors (e.g., [154, 155]) have obtained good fits of experimental data with the Langmuir isotherm, and there has been at least one report of sensor response being exponential in target concentration [156]. One complicating factor is whether the binding is controlled kinetically or reaches equilibrium during the experiment.

Understanding the exact nature of the θ([Target]) and $\Delta Z(\theta)$ transfer functions could lead to improvements in affinity biosensors and would enable greater understanding of impedance change mechanisms. Some investigators attempt to independently measure target surface coverage using techniques such as QCM or SPR or label-based techniques (e.g., [157, 158]).

There is no standardized method for determining biosensor dose-response curves [151], and the lack of reproducibility further confounds this issue. Investigators with flow-through apparatus often use successive injections of target, with binding assumed to be cumulative and irreversible [46]. Other methods may introduce variation by regenerating the probe layer between experiments or using completely different sensors for different points on the response curve. This latter method is expected to capture the most non-reproducible behavior but may most closely represent biosensor performance in the real world.

5.3. Differential Measurement

Utilizing a differential measurement scheme can eliminate variations in the sensor output caused by disturbances unrelated to the sensed quantity. For example, R_{sol} and C_{surf} are affected by salt concentration, pH, and temperature; impedance changes due to uncontrolled changes of these factors may swamp out the tiny impedance change caused by target-probe binding. In complex samples, nonspecific binding is also expected to give a response unrelated to target concentration.

To compensate, a *reference sensor* can be used. Ideally, no target binding occurs on the reference sensor but otherwise it has an identical response to the solution. The signal then consists of the difference between the working and reference sensor responses, hopefully eliminating any *common-mode* signal due to extraneous environmental factors. However, the differential response may contain contributions from common-mode changes due to imperfect matching. The less controlled the sample to be measured, the more difficult it is to select a reference *probe* coating and ensure cancellation of other effects. Making an impedance measurement before and after target binding, while attempting to make every other impedance-determining variable the same, could also be considered a differential measurement in some sense. Particularly if working and reference sensors react similarly to nonspecific binding, differential schemes can enhance both selectivity and sensitivity of the overall system [90, 159].

5.4. Self-Assembled Monolayers

As we have seen, the affinity aspect is often the limiting factor label-free biosensor performance. Thus, it is critical that the probe molecule be attached to the sensor surface in a way that maintains probe specificity and activity while inhibiting nonspecific binding. We cannot fully review biosensor surface chemistry here, but give a few results relevant to impedance biosensors.

Most impedance biosensors utilize self-assembled monolayers (SAMs) to attach probes at the electrode-solution interface. The most common types of attachment chemistries are based on thiols bound to gold surfaces [160] and siloxanes to oxide surfaces [161]. Here, we focus on thiol SAMs because they are prevalent in impedance biosensors. The SAM can be formed and the probes subsequently immobilized on top or else the probes themselves can be thiol-modified and formed as a SAM (usually with a thiol diluent to ensure adequate probe spacing).

For nonfaradaic sensors a tightly-packed (high R_{leak}) SAM is desirable, in contrast with faradaic sensors where the electrode surface needs to be accessible to the redox species but not to adsorption of other molecules [162]. SAMs with longer carbon chains form more dense monolayers due to hydrophobic interactions of the chains. The general rule of thumb is that C_{11} or greater gives packed films [163, 164], but Mirksy et al. reported C_{surf} drift due to thiol desorption using a C_{11} SAM but not for a C_{16} SAM [154, 165]. SAM desorption is one reason why a sensor might have a response to a blank solution. Boubour reported that over 40 hours of incubation was required to form a tightly-packed SAM, as determined by observing purely capacitive behavior at low frequencies [166], but others report 15 – 20 hours depending on SAM composition [167] and as little as 2 hours [162].

It is important to remember that SAMs are only good electrical insulators over a window of DC bias voltages, depending on the terminal group and chain length. For gold-thiol SAMs with hydrophilic headgroups, DC conduction

(i.e. finite R_{leak}) was noted even at 0 V bias vs. Ag/AgCl with a C_{16} SAM in the absence of a redox species [168]. This is likely due to voltage-induced structural rearrangement of the SAM that results in pinholes [169] or permeation of SAM with ions or water molecules [170]. Extreme DC bias voltages can actually oxidize or reduce the bonds between a metal electrode and biological probe layer (reported values for gold-thiol are summarized in [166]). This effect has been utilized to selectively functionalize electrodes [171–174]. Air exposure can also oxidize the thiol-gold bonds [132].

Lai et al. recently published an important report of SAM stability during dry storage; they concluded that longer SAMs are more stable and that preservatives can insure stability over one month with reproducible results [162]. The hexacyanoferrate(II/III) redox couple used almost universally in faradaic impedance sensors can degrade the electrode-SAM interface over time, particularly when exposed to light [175, 176], and also reduces the activity of peptide probe layers [177].

5.5. DNA vs. Protein Biosensors

Using oligonucleotides (most often DNA) as probes and targets may be somewhat more convenient than using antibodies or other proteins. Oligonucleotides are readily available in purified form, immobilization chemistry is relatively mature, and hybridization exhibits relatively robust selectivity. However, it is unclear whether impedance DNA biosensors have any commercial viability because various detection technologies already exist for DNA (e.g., DNA microarrays, pyrosequencing, real time polymerase chain reaction), and other technologies are being researched (e.g., voltammetry using redox-labeled DNA). However, DNA-based sensors can demonstrate proof-of-principle for protein impedance biosensors and elucidate properties of the electrode/solution interface. Additionally, a market may exist for inexpensive and portable impedance-based DNA diagnostics where moderate sensitivity is sufficient.

Aptamers are oligonucleotide or peptide sequences which bind selectively to a desired target, including proteins [178, 179]. They are chosen by an in vitro selection process that identifies a monomer sequence that tightly binds the target from a large library of random sequences [180, 181]. Aptamers are considered promising alternatives to antibodies for capture probes because of facile production, well-understood tethering chemistry, and perhaps reduced cross-reactivity [182].

As already mentioned briefly in Section 2.1, protein detection appears to be the more likely real-world application of affinity impedance biosensors because (1) labeling proteins is difficult and impedance sensing can be label-free and (2) difficulties in cross-reactivity and nonspecific binding severely impact all protein sensors, allowing less sensitive readout techniques to be utilized with equal overall results (i.e. the affinity step might dictate the detection limit rather than the readout step). Only moderate levels of multiplexing are practical for protein assays, a good fit with the moderate levels of multiplexing easily achievable with impedance biosensors.

Most published reports use target proteins of real-world interest but in highly purified conditions; much effort is still required to bring about robust analysis of clinical samples using impedance biosensors which will enable point-of-care applications. Key issues include poor reproducibility, nonspecific binding, and the complex and highly variable nature of clinical samples. Some protein sensors are termed *immunosensors* in the primary literature because they detect antibodies or antigens; antibodies and most antigens are proteins so we make no distinction here.

If an antigen is used as the probe, target antibodies can be detected. Judged on a per molecule basis, these reverse arrays [183] could be more sensitive than using a large capture antibody to detect a small protein if measured impedance depends on target size. These sorts of antibody sensors could be useful for allergen screening and for detecting autoimmune disorders.

6. Summary of Published Label-Free Affinity Impedance Biosensors

Here we summarize the results of many researcher's efforts. Although we have made every attempt to thoroughly review the relevant literature through the end of 2006, some meritorious publications may have been overlooked. Table 1 contains a summary of selected label-free affinity impedance biosensors for quick comparison, but the text summarizes many additional reports.

It is interesting to note that reported detection limits have not systematically improved with time. We speculate that reasons might include limitations in the affinity step, different definitions of the limit of detection, limitations related to common-mode disturbances, and increased awareness of challenges related to sensor reproducibility.

6.1. Early Affinity Impedance Biosensors

Credit for the first capacitive affinity biosensor is widely given to Newman [184], who in 1986 used interdigitated electrodes covered by insulation and an antibody probe. In 1988, Taylor et al. reported an impedimetric sensor for the small molecule acetylcholine and a related neurotoxin using protein receptors isolated from animal tissue [21]. Interdigitated gold electrodes were coated with a polymer, either with or without the receptor, and a bridge configuration was used to detect the differential impedance change. Several years later with very similar apparatus, they reported detection of as little as 50 ng/mL of antibody hIgG [185].

Many early impedance biosensors were based on a metal or semiconductor coated with a thin layer of native oxide to which the probes were attached. Some of these sensors worked at least partially on field-effect principles, which are not considered here. Using a thin native oxide on doped

Table 1. Summary of selected label-free affinity impedance biosensors for comparison. Detection limits are estimated if not explicitly stated in the publication.

Probe	Target	LoD	Measurement	Var.	Excitation	Surface Chemistry	Reference	Year	Cit.	Comments
antibody	hlgG	50 ng/mL	ID-electrode nonfaradaic	Z @ freq	100 Hz?	polymer/probe mix	electrode w/ or w/o Ab	1991	[185]	one of first affinity impedance biosensors
antibody	IgG, anti-IgG	est. <1 ng/mL	2-electrode nonfaradaic	C_{surf}	100 mV @ 1 kHz	silane, linker	after-before, time course	1992	[133]	significant nonspecific binding
antibody	α-fetoprotein	est. 50 ng/mL	2-electrode nonfaradaic	Z @ freq	1.5 kHz	silane, linker	IgG-coated electrode	1997	[187]	SiO_2 surface biased so no field-effect
antibody	HSA	1000 ng/mL	2-electrode nonfaradaic	C_{surf}	10 mV @ 20 Hz	various compared	time course	1997	[154]	results with HDA + linker, normalized
antibody	IL-2	est. 0.05 ng/mL	3-electrode nonfaradaic	C_{surf}	50 mV step	SAM, linker, C12 diluent	after-before	1998	[149]	several other Ab-target pairs tried
antibody	interferon-γ	0.00000002 ng/mL	3-electrode nonfaradaic	Z @ freq	10 mV @ 113 Hz	SAM, linker	time course	2001	[196]	flow system, large nonspecific signal
antibody	Schistosoma japonicum	0.1 ng/mL	3-electrode nonfaradaic	C_{surf}	50 mV step	PrA linker, thiol diluent	after-before, time course	2002	[191]	optimized several parameters
antibody	IgG	100 ng/mL	3-electrode nonfaradaic	Z @ freq	10 mV @ 10 kHz	conducting polymer entrapment	blank-coated electrode	2002	[90]	
antibody	vitellogenin	420 ng/mL	3-electrode nonfaradaic	R_{ct}	10 mV @ $10-10^5$ Hz	conducting polymer, linker	after-before	2004	[206]	redox species in polymer
antibody	HSA	1.6 ng/mL	3-electrode nonfaradaic	Z @ freq	10 mV @ 34 Hz	polymer, linker	after-before	2005	[150]	optimized several parameters
antibody	transferrin	0.08 ng/mL	3-electrode faradaic	C_{surf}	50 mV step	Au nanoparticles, conducting polymer	after-before, time course	2005	[194]	significant nonspecific binding
antibody	α-fetoprotein	10000 ng/mL	3-electrode nonfaradaic	C_{surf}	50 mV step	various compared	after-before	2006	[190]	similar results for all surface chemistries
antigen	anti-HRP	0.024 ng/mL	3-electrode faradaic	C_{surf}	10 mV @ $0.05-10^4$ Hz	SAM, linker	after-before	2005	[203]	includes some SPR data
antigen	anti-Der 12	est. 2000 ng/mL	3-electrode faradaic	R_{ct}	5 mV @ $10^{-1}-10^5$ Hz	MPTS, Au nanoparticles	after-before	2006	[208]	Au deposited on GCE
antigen	antibody	0.00 ng/mL	3-electrode nonfaradaic	C_{surf}	50 mV step	thiol-probe, C16 diluent	after-before	2006	[193]	reverse array to test probe composition
aptamer	lysozyme	est. 1000 ng/mL	3-electrode faradaic	R_{ct}	5 mV @ $10^{-2}-10^5$ Hz	ITO, SA, biotin-aptamer	after-before	2005	[116]	
aptamer	IgE	19 ng/mL	3-electrode faradaic	R_{ct}	5 mV @ 10^3-10^5 Hz	SAM, linker		2005	[201]	small electrode array
aptamer	thrombin	3.6 ng/mL	3-electrode faradaic	R_{ct}	5 mV @ $1-10^5$ Hz	thiol-probe, C6 diluent	after-before	2006	[117]	
ssDNA	ssDNA	0.0000000002 nM	3-electrode nonfaradaic	C_{surf}	50 mV step	thiol-DNA, C2 diluent	after-before, time course	1999	[188]	with very long target, large nonspecific signal
ssDNA	ssDNA	4 nM	3-electrode faradaic	R_{ct}	10 mV @ $10^{-2}-10^5$ Hz	silane, Ag nanoparticle	after-before	2005	[209]	
ssDNA	ssDNA	100 nM	3-electrode nonfaradaic	R_{ct}	10 mV @ $0.5-10^5$ Hz	polymer	after-before	2005	[207]	significant nonspecific binding

silicon and biasing the silicon to the strong accumulation region (insuring that field effects were negligible), Maupas et al. were unable to detect impedance changes using a silane-antibody coupling but observed significant changes in the impedance of a polymer-antibody film when exposed to α-fetoprotein target, with a detection limit of 10 – 20 ng/mL [186]. Subsequently, using antibody-functionalized platinum electrodes, they reported a detection limit of ca. 100 ng/mL for α-fetoprotein by measuring the differential impedance changes at 1.5 kHz [187]. Though nonspecific binding of serum proteins greatly reduced sensitivity (limitation of the affinity step), they claimed reproducible impedance changes on the order of 1%. Gebbert et al. used a electrochemically-grown tantalum oxide with controlled thickness as an insulator, and were able to detect anti-mouse-IgG to 1 ng/mL levels with mouse-IgG as a probe by measuring capacitance at 1 kHz in real time, though nonspecific binding was significant [133].

6.2. Potentiostatic Step

Lund University researchers pioneered the use of the potentiostatic step technique for impedance biosensors; a voltage step is applied and the resulting current is fit to a simple *RC* model (using R_{sol} and C_{surf}). The instrumentation is described in [94, 135]. Relatively low electrolyte concentrations and a fast potentiostat are required to capture the initial part of the curve. Any CPE behavior of the interface is neglected. However, a complete measurement may be made quite rapidly.

In 1997 Berggren reported an impressive detection limit of 0.5 pg/mL for the protein hCG, noting that sensors with probes for two other antigens (HSA and IL-2) gave much smaller responses [111]. In 1998 similar results were reported for IL-2, and even more impressive results for IL-6, though the detection limits were not specified [149]. The same investigators later constructed a DNA biosensor based on the same principle, and reported a detection limit of 0.2 aM for a 179mer ssDNA target using 26mer and 8mer oligonucleotide probes [188]. They used a target much larger than the probe, but a still-impressive 1 – 5 aM limit of detection is expected for identical-length targets. However, there was a large nonspecific binding signal for unrelated DNA, and reproducibility was poor. A hiatus ensued, but recently results have been published with much higher detection limits. In 2005 they described a continuous monitoring of human serum albumin for bioprocess monitoring, where greatly reduced sensitivity is adequate (measurement range was well above 10 μg/mL) [189]. Collaborating researchers Limbut et al. experimented with three different surface chemistries for antibody immobilization, and obtained roughly 10 μg/mL detection limits for the α-fetoprotein target in each case [190].

Other investigators have used the same measurement approach. In 2002 Zhou et al. reported an impressive detection limit of 0.1 ng/mL for an antibody-based sensor for a protein disease marker, but unfortunately there were no follow-up publications [191]. Jiang et al. used faradaic EIS measurements to validated the simple *RC* model used for potentiostatic step readout and then used the latter to detect a protein using an antibody capture agent, claiming a detection limit of 10 ng/mL [192]. In an excellent recent paper, Zhang et al. detected trace impurities of an enantiomeric drug by tethering the small molecule to be detected as the probe layer, taking advantage of the comparatively large size of the antibody recognition agent (one disadvantage is such a sensor cannot be prepared beforehand) [193]. They demonstrate good reproducibility and low nonspecific response, and report an absolute detection limit of 5 pg/mL as well as detecting a 10 ppm enantiomeric impurity. Other reports using the potentiostatic step method include Jiang [110] and Hu [194] (both detailed in Sect. 6.6), and Wang et al. who claim a 2.5 pg/mL limit of detection for low-weight protein r-HV2 using a faradaic measurement [195].

6.3. Nonfaradaic Studies

In 1997 Mirsky et al. used anti-HSA antibodies attached to a tightly packed SAM, collecting data at 20 Hz where the impedance was purely capacitive [154]. Notably, they monitored the capacitance change during probe immobilization in order to estimate probe density, and were thus able to normalize the subsequent impedance change (upon target binding) and improve response reproducibility (10 – 30% over several trials). Though the reported detection limit is very modest (1 μg/mL), the paper demonstrates an understanding of the issues that need to be addressed. Slightly earlier, Rickert et al. reported detecting antigen capture of an antibody using both faradaic and nonfaradaic measurements of C_{surf} and concluded that nonfaradaic was preferable. They observed significant nonspecific binding and drift, but the initial change in C_{surf} allowed detection to μg/mL levels [177].

Ma et al. recently reported significant (10 – 20%) impedance changes upon target DNA hybridization compared with negligible changes on the nonspecific control electrode using nonfaradaic EIS [78] (subsequently they attempted amplification with disappointing results). Target concentrations were very high so no detection limit was determined.

Lasseter et al. measured impedance of biotin-functionalized surfaces upon avidin binding over a very wide frequency range in a nonfaradaic scheme [157]. They observed that the main impedance change occurred at frequencies so low (<1 Hz) that the R_{leak} was the main affected equivalent circuit element; this indicates that perhaps the binding might be more readily detected using faradaic EIS.

In 2001 Dijksma et al. published work reporting the unprecedented detection limit of 0.02 fg/mL for protein interferon-γ using a nonfaradaic measurement of an antibody-modified SAM [196]. Like some other investigators, they made use of a flow cell and introduced controlled amounts of antigen followed by buffer washes. Although

they reported significant nonspecific binding, they found that it could be largely corrected by subsequent washing steps. A follow-up study replicated these results and independently verified from signal-to-noise considerations that the optimal measurement frequency had previously been used [151]. Their idea of determining the binding signal-to-noise ratio at different frequencies is a powerful concept. Like the original study, repeatability and nonspecific response were somewhat problematic. Interestingly, a positive DC bias of 200 mV increased the sensor response.

6.4. Faradaic Studies

Faradaic impedance biosensors almost always monitor changes in R_{ct} when affinity binding occurs. Liu et al. reported a DNA sensor based on faradaic impedance spectroscopy and were able to easily detect 1 nM of 15mer target [155]. The observed change in R_{ct} is presumably due to electrostatic repulsion between the negatively-charged redox species and negative charge on the DNA. Probes were made of PNA, a DNA mimic with a neutral backbone, to increase fractional R_{ct} change.

The Lee and Kraatz group have published a series of papers demonstrating that mismatched DNA can be distinguished from perfectly matched dsDNA by differences in R_{ct} between different DNA conformations (which can be selected based on ion concentrations and pH) [115, 197, 198]. They also detected mismatches by changes in R_{ct} when the mismatch-binding-protein MutS was introduced [199]. Akagi et al. recently demonstrated discrimination of single nucleotide polymorphisms (mismatch of a single base pair) by extending the probe strand via ligation and measuring resulting change in R_{ct} arising from that extension rather than from the hybridization itself. Although this adds extra steps (contrary to the spirit of label-free detection), they claim detection limits in the pg/mL range, or much less than 1 nM [200].

Xu et al. published a report using aptamer probes on a small array of electrodes which were interrogated using faradaic EIS [201]. Upon binding of the IgE target, R_{ct} increased significantly. Sensitivity using aptamer probes was higher than using antibody probes. The sensor showed good reproducibility and the multiplexed setup makes it possible to include reference electrodes for differential measurement. They estimated a 0.1 nM (ca. 20 ng/mL) limit of detection.

Cai et al. reported a thrombin sensor using an aptamer probe on a microfabricated gold electrode [117]. They noted increases in R_{ct} and hypothesize that thrombin acts as a hydrophobic insulator (however, it is positively charged and the redox species is negatively charged). Using three replicates, they reported no nonspecific binding of hemoglobin or BSA and a detection limit of 3.6 ng/mL. Ding et al. noticed an increase in R_{ct} accompanied by a tiny decrease in C_{surf} using μg/mL concentrations of biotin exposed to an avidin-functionalized gold electrode, and reported a detection limit of 20 ng/mL [118]. In contrast with these two reports, Rodriguez et al. noted a decrease in R_{ct} upon target binding to an aptamer probe [116]. This was explained by the fact that the target had a significant positive charge but the probe was negatively charged, and thus target binding decreased the electrostatic barrier for the negative redox species. Taken together, these studies demonstrate that competing effects determine ΔR_{ct}, implying that this detection strategy may not be generalizable.

Ameur et al. used a SAM-functionalized gold electrode in a flow cell with various routes to antibody immobilization in an early faradaic study [202]. They reported detection limits of 5 – 10 pg/mL depending on functionalization route. Pyun et al. recently reported the use of a flow cell with faradaic measurement [203]. Few details of the actual data or analysis are provided, but they assert that changes in C_{surf} allowed quantification of an antibody over an enormous dynamic range, from the detection limit of 24 pg/mL upwards 6 orders of magnitude. Because C_{surf} is being measured, a nonfaradaic measurement also should be possible. Likewise, Hays et al. used a faradaic measurement to detect hemoglobin binding at functionalized electrodes [158]. The impedance change was primarily in the imaginary component of low frequency impedance, suggesting that C_{surf} was the principal model element affected and could be measured by nonfaradaic means.

6.5. Polymer Films

One approach to electrode functionalization is to use polymer films to which biomolecular probes can be attached or entrapped [204]. Either faradaic or nonfaradaic measurement can subsequently be employed. Often the deposited polymer contains redox centers or is semiconducting, in which case it may act as an extension of the metal electrode.

The earliest impedance biosensors by Newman [184] and Taylor [21] used nonconducting polymer films. In 2001 Lillie et al. observed changes in phase angle at low frequencies when a conducting polymer film with embedded antibodies was exposed to luteinizing hormone, allowing detection in a clinically-relevant concentration range [205]. Sadik compared various polymer functionalization chemistries with a differential system and reported a detection limit of 100 ng/mL for target IgG, though lower detection limits were observed for cyanazine-BSA target if a very large AC excitation was used [90]. More recently, Wu et al. used a thin insulating polymer to create a nonfaradaic capacitive sensor [150]. They achieved the impressive detection limit of 1.6 ng/mL for the HSA target after optimizing antibody density, pH, and measurement frequency, and also showed evidence for excellent reproducibility and selectivity against nonspecific binding.

Darain et al. used a conducting polymer film to detect a fish sex biomarker; no external redox species was added but the R_{ct} of the polymer film itself was found to depend on target binding and allowed detection down to 0.42 μg/mL in pure samples and discrimination of fish sex using serum samples [206]. Ouerghi et al. demonstrated response of a

conducting polymer coated with antibodies to IgG concentrations in the range 10 – 80 ng/mL in nonfaradaic conditions at very low frequencies, though no blank solution or nonspecific target was tested [156]. Tlili et al. utilized a very similar approach with a ssDNA probe detect complementary DNA down to 100 nM [207]. Changes in the electrical properties of a conducting polymer were the proposed explanation in an antibody sensor [143] and DNA hybridization sensor [144].

6.6. Special Electrode Surfaces

Recently, several researchers have attempted to increase electrode surface area in order to increase the number of attached probes and therefore increase the sensitivity. Li et al. deposited gold electrochemically from solution onto an electrode for a faradaic impedance sensor that detected a DNA intercalating drug by noting changes in R_{leak} in parallel to the SAM in the fit model [134]. Huang et al. used faradaic EIS with an allergen probe immobilized on an electrode coated with gold nanoparticles to detect antibodies in the range of 10 s of μg/mL via increased R_{ct} [208]. A similar approach with silver nanoparticles was used by Fu et al. to detect DNA down to 4 nM [209]. Hu et al. used gold nanoparticles loaded on top of a polymer-coated electrode to immobilize antibodies [194]. With a potentiostatic step readout they were able to detect transferrin concentrations ranging from 80 pg/mL to 100 ng/mL, though the sensor showed over 10% nonspecific response.

Jiang et al. used alumina sol-gel surface with antibodies detected hIgG and two liver fibrosis markers [110] using a potentiostatic step method. The reported limit of detection was about 1 ng/mL for individual analytes. Notably, cross-reactivities were explicitly tested and were below 10% except at concentrations below 10 ng/mL, where they were worse.

DeSilva et al. published an early report using a film of platinum islands coated with an antibody probe as the sensor surface [210] with impedance readout at 100 Hz. Although the reported 0.4 ng/mL limit of detection is impressive, only three sensor surfaces were measured thus little characterization of the nonspecific response could be performed. A similar approach was undertaken by Pak in 2001 [211] with similar limitations, but to the authors' knowledge this approach has not been pursued recently.

6.7. Interdigitated Electrodes

As already mentioned, the earliest capacitive biosensors were based on interdigitated electrodes (IDEs) [21, 184, 185], which are easily fabricated by conventional microfabrication techniques and are used for sensors and other applications [212]. The impedance measured is between the two electrodes, and often no explicit electrical connection is made with the solution, a major difference between them and the other types of impedance biosensors mentioned in this review. Depending on geometry, the inter-electrode capacitance can degrade sensitivity to changes at the electrode-solution interface. While not a label-free approach, conductometric amplification using silver deposition (see Sec. 3.6) typically uses exposed interdigitated electrodes.

Interdigitated electrodes for label-free affinity biosensing are still being explored. Laureyn et al. characterized IDEs with nanoscale fingers and reported an impedance change during probe immobilization but did not report on target binding [213]. Hang et al. described changes in impedance between Pt IDEs upon DNA hybridization [214]. Very large DNA concentrations were used. Interestingly, they noted that the R_{sol} component varied the most upon hybridization, not C_{surf}.

6.8. Miniaturization Efforts

In an attempt to miniaturize impedance/capacitance biosensors, several researchers have attempted to create integrated circuits to perform the measurement. One of these approaches is to determine the charge required to bring the interface to a particular voltage, implicitly measuring the capacitance. This technique neglects many intricacies of the actual interface impedance (e.g., voltage dependence of C_{surf}, R_{leak}) but is simple to implement; significant impedance changes have been observed in both discrete [215] and integrated [216, 217] implementations. Although high concentrations of target DNA were used and relatively little reproducibility data is presented, this is a promising line of research. Recently an integrated multipurpose electrochemical sensor for biomolecular detection was presented; while impressive electrical performance was achieved, very few measurements with a biofunctional surface were reported [159, 218].

7. Conclusions and Research Directions

It has been repeatedly demonstrated that protein and DNA binding to immobilized probes is detectable by measuring impedance changes at electrode-solution interfaces, but there are many aspects requiring further refinement. Some of these issues are applicable to all affinity biosensors regardless of readout technology, while others are unique to impedance readout. Both the affinity and the readout steps impact the limit of detection. Some investigators report sub-ng/mL limits of detection while other investigators report figures orders of magnitude higher. There has been no systematic improvement in reported detection limits during the past 15 years of label-free affinity biosensor research.

Arguably the most daunting issue facing affinity biosensors in general is the problem of selectivity even in the presence of large concentrations of nontarget material. This obstacle can be overcome by using labels and/or labeled secondary probes. However, both of these solutions are contrary to the goal of creating a point-of-care detection

device because they require extra time, add extra sample preparation steps, and increase overall system complexity. This challenge is common to all label-free affinity sensors, no matter what readout method is used.

Therefore, we suggest that investigators devote increased attention to the nonspecific response of their sensors, and demonstrate selectivity to the chosen analyte in the presence of large background concentration of nonspecific interferents. A first step towards this goal is reporting the sensor response to a large concentration of nontarget, testing specificity. A second step is to include a small concentration of target in a background of nontarget. We suggest that investigators begin to routinely report such data, anticipating applications where this will be more important than the clean limit of detection. We applaud authors who include nonspecific binding data in publications, even if it appears unfavorable.

Researchers should validate their reported detection limit by showing that the sensor response to blank and target solutions is significantly different over multiple trials. Furthermore, we suggest that reproducibility data be explicitly presented, such as by giving coefficient of variance of multiple experiments (ideally on different days using different sensors). The methodology for determining the response curve should be stated and reproducibility data presented clearly along with it.

Mechanisms by which the affinity interaction changes the measured interface impedance are poorly understood. There is need for both experimental and theoretical work in this regard, and challenge is confounded by the more general problem of assigning measured impedance to a particular physical phenomenon. To date, most publications briefly present a plausible explanation for the measured ΔZ which is supported by their observations but never tested independently. Comprehensive studies of a particular impedance change model with different probe/target combinations to verify predicted trends would be valuable. With an understanding of the molecular mechanisms underlying impedance change, the optimal conditions and an optimal measurement approach can be chosen rationally (e.g., faradaic measurement of ΔR_{ct} or nonfaradaic measurement of ΔC_{surf}).

A need exists for a thorough theoretical treatment of scaling effects in impedance biosensors (see Sec. 4.9). Electrode size impacts the required measurement frequency range, and measurement accuracy depends on measurement frequency and instrumentation design. Optimizing electrode size may allow smaller impedance changes to be reliably detected, which may lower the detection limit.

Instrumentation is lacking for sensor arrays and for handheld point-of-care applications. Only limited progress has been made in implementing arrays of affinity impedance sensors. However, sensor arrays are valuable for several reasons. First, redundancy can be built-in by having multiple sensors dedicated to a single target, with the individual sensor responses combined to improve reproducibility and accuracy. Second, if different sensors are used to detect different targets then a panel of biomarkers can be assayed simultaneously; this is advantageous for disease diagnosis and reduces cost and sample volume per data point. To date, virtually all published affinity impedance sensors are based on bulky single-channel EIS instrumentation. Only limited efforts have been expended in miniaturization of the electronics for point-of-care applications, though extensive development may be premature.

Publications should clearly establish the context of prior related work and compare results with others', even if performance is inferior [219]. In 2005 Kissinger proposed several criteria for high-quality biosensor publications, including demonstration of utility in the proposed application conditions (including nontarget background and relevant concentration levels), and made insightful comments on the state of biosensor research [220].

After two decades of research effort and hundreds of publications, no product based on label-free affinity impedance-based biosensors has enjoyed widespread commercial success. While some progress can come by simply optimizing existing affinity impedance biosensors, larger problems remain. Some of these challenges are in the biological realm (affinity step), and some are in the physical realm (readout step), but all need to be solved in context of the entire system. Future research in the area of label-free affinity biosensors should be targeted towards applications that leverage the techniques' advantages (low cost, small size, low power, simplified sample preparation, and moderate multiplexing capability) without requiring exquisite sensitivity.

8. Acknowledgements

The authors acknowledge support from the National Human Genome Research Institute (HG000205/HG/NHGRI and T32 HG00044/HG/NHGRI).

9. References

[1] D. R. Thévenot, K. Toth, R. A. Durst, G. S. Wilson, *Biosens. Bioelectron.* **2001**, *16*, 121.
[2] T. G. Drummond, M. G. Hill, J. K. Barton, *Nat. Biotechnol.* **2003**, *21*, 1192.
[3] E. Bakker, *Anal. Chem.* **2004**, *76*, 3285.
[4] J. R. Macdonald, *Impedance Spectroscopy: Emphasizing Solid Materials and Systems*, Wiley, New York **1987**.
[5] M. J. Schoning A. Poghossian, *Electroanalysis* **2006**, *18*, 1893.
[6] M. J. Schoning, A. Poghossian, *Analyst* **2002**, *127*, 1137.
[7] G. F. Zheng, F. Patolsky, Y. Cui, W. U. Wang, C. M. Lieber, *Nat. Biotechnol.* **2005**, *23*, 1294.
[8] A. Star, E. Tu, J. Niemann, J. C. P. Gabriel, C. S. Joiner, C. Valcke, *PNAS* **2006**, *103*, 921.
[9] P. Bataillard, F. Gardies, N. Jaffrezic-Renault, C. Martelet, B. Colin, B. Mandrand, *Anal. Chem.* **1988**, *60*, 2374.
[10] J. Fritz, E. B. Cooper, S. Gaudet, P. K. Sorger, S. R. Manalis, *PNAS* **2002**, *99*, 14142.

[11] K. Y. Tse, B. M. Nichols, W. S. Yang, J. E. Butler, J. N. Russell, R. J. Hamers, *J. Phys. Chem. B* **2005**, *109*, 8523.
[12] P. Estrela, P. Migliorato, H. Takiguchi, H. Fukushima, S. Nebashi, *Biosens. Bioelectron.* **2005**, *20*, 1580.
[13] F. Bendriaa, F. Le-Bihan, A. C. Salaun, T. Mohammed-Brahim, C. Tlili, N. Jaffrezic, H. Korri-Youssoufi, *2005 IEEE Sensors* **2005**, 412.
[14] J. C. Owicki, L. J. Bousse, D. G. Hafeman, G. L. Kirk, J. D. Olson, H. G. Wada, J. W. Parce, R. M. Stroud, *Ann. Rev. Biophys. Biomol. Struct.* **1994**, *23*, 87.
[15] A. Poghossian, T. Yoshinobu, A. Simonis, H. Ecken, H. Luth, M. J. Schoning, *Sens. Actuators, B* **2001**, *78*, 237.
[16] A. Poghossian, A. Cherstvy, S. Ingebrandt, A. Offenhausser, M. J. Schoning, *Sens. Actuators, B* **2005**, *111 – 112*, 470.
[17] A. Zebda, V. Stambouli, M. Labeau, C. Guiducci, J. P. Diard, B. Le Gorrec, *Biosens. Bioelectron.* **2006**, *22*, 178.
[18] W. Cai, J. R. Peck, D. W. van der Weide, R. J. Hamers, *Biosens. Bioelectron.* **2004**, *19*, 1013.
[19] H. Berney, J. Alderman, W. Lane, J. K. Collins, *Sens. Actuators, B* **1997**, *44*, 578.
[20] V. Billard, C. Martelet, P. Binder, J. Therasse, *Anal. Chim. Acta* **1991**, *249*, 367.
[21] R. F. Taylor, I. G. Marenchic, E. J. Cook, *Anal. Chim. Acta* **1988**, *213*, 131.
[22] I. Bontidean, C. Berggren, G. Johansson, E. Csoregi, B. Mattiasson, J. A. Lloyd, K. J. Jakeman, N. L. Brown, *Anal. Chem.* **1998**, *70*, 4162.
[23] F. Yin, *Anal. Lett.* **2004**, *37*, 1269.
[24] S. Hleli, C. Martelet, A. Abdelghani, N. Burais, N. Jaffrezic-Renault, *Sens. Actuators, B* **2006**, *113*, 711.
[25] L. J. Yang, Y. B. Li, C. L. Griffis, M. G. Johnson, *Biosens. Bioelectron.* **2004**, *19*, 1139.
[26] S. M. Radke, E. C. Alocilja, *IEEE Sens. J.* **2005**, *5*, 744.
[27] I. O. K'Owino, O. A. Sadik, *Electroanalysis* **2005**, *17*, 2101.
[28] N. N. Mishra, S. Retterer, T. J. Zieziulewicz, M. Isaacson, D. Szarowski, D. E. Mousseau, D. A. Lawrence, J. N. Turner, *Biosens. Bioelectron.* **2005**, *21*, 696.
[29] M. Stelzle, G. Weissmuller, E. Sackmann, *J. Phys. Chem.* **1993**, *97*, 2974.
[30] W. Knoll, F. Yu, T. Neumann, S. Schiller, R. Naumann, *Phys. Chem. Chem. Phys.* **2003**, *5*, 5169.
[31] E. Katz, I. Willner, *Electroanalysis* **2003**, *15*, 913.
[32] C. Berggren, B. Bjarnason, G. Johansson, *Electroanalysis* **2001**, *13*, 173.
[33] A. J. Bard, L. R. Faulkner, *Electrochemical Methods: Fundamentals and Applications*, Wiley, New York **2001**.
[34] P. Bergveld, *Biosens. Bioelectron.* **1991**, *6*, 55.
[35] A. Warsinke, A. Benkert, F. W. Scheller, *Fresenius J. Anal. Chem.* **2000**, *366*, 622.
[36] J. J. Gooding, *Electroanalysis* **2002**, *14*, 1149.
[37] R. Moeller, W. Fritzsche, *IEE Proc. Nanobiotech.* **2005**, *152*, 47.
[38] J. Wang, *Biosens. Bioelectron.* **2006**, *21*, 1887.
[39] A. Rasooly, *Biosens. Bioelectron.* **2006**, *21*, 1847.
[40] A. Rasooly, J. Jacobson, *Biosens. Bioelectron.* **2006**, *21*, 1851.
[41] B. B. Haab, *Proteomics* **2003**, *3*, 2116.
[42] K. R. Rogers, *Mol. Biotech.* **2000**, *14*, 109.
[43] U. Bilitewski, *Anal. Chim. Acta* **2006**, *568*, 232.
[44] R. A. Goldsby, T. J. Kindt, B. A. Osborne, *Immunology*, W. H. Freeman, New York **2003**.
[45] P. Skladal, *Electroanalysis* **1997**, *9*, 737.
[46] R. Karlsson, P. S. Katsamba, H. Nordin, E. Pol, D. G. Myszka, *Anal. Biochem.* **2006**, *349*, 136.
[47] P. Schuck, R. M. Stroud, *Ann. Rev. Biophys. Biomol. Struct.* **1997**, *26*, 541.
[48] C. K. O'Sullivan, G. G. Guilbault, *Biosens. Bioelectron.* **1999**, *14*, 663.
[49] C. Ziegler, *Anal. Bioanal. Chem.* **2004**, *379*, 946.
[50] J. Homola, S. S. Yee, G. Gauglitz, *Sens. Actuators, B* **1999**, *54*, 3.
[51] M. A. Cooper, *Anal. Bioanal. Chem.* **2003**, *377*, 834.
[52] R. P. Ekins, *Clin. Chem.* **1998**, *44*, 2015.
[53] D. Leech, *Chem. Soc. Rev.* **1994**, *23*, 205.
[54] A. W. Peterson, R. J. Heaton, R. M. Georgiadis, *Nucleic Acids Res.* **2001**, *29*, 5163.
[55] A. Vainrub, B. M. Pettitt, *Phys. Rev. E* **2002**, *66*, 041905.
[56] G. Bhanot, Y. Louzoun, J. H. Zhu, C. DeLisi, *Biophys. J.* **2003**, *84*, 124.
[57] P. E. Sheehan, L. J. Whitman, *Nano Lett.* **2005**, *5*, 803.
[58] W. Kusnezow, Y. V. Syagailo, S. Ruffer, N. Baudenstiel, C. Gauer, J. D. Hoheisel, D. Wild, I. Goychuk, *Mol. Cell Prot.* **2006**, *5*, 1681.
[59] J. Vessman, R. I. Stefan, J. F. Van Staden, K. Danzer, W. Lindner, D. T. Burns, A. Fajgelj, H. Muller, *Pure Appl. Chem.* **2001**, *73*, 1381.
[60] I. M. Thompson, D. K. Pauler, P. J. Goodman, C. M. Tangen, M. S. Lucia, H. L. Parnes, L. M. Minasian, L. G. Ford, S. M. Lippman, E. D. Crawford, J. J. Crowley, C. A. Coltman, Jr., *N. Engl. J. Med.* **2004**, *350*, 2239.
[61] L. Maattanen, A. Auvinen, U. H. Stenman, T. Tammela, S. Rannikko, J. Aro, H. Juusela, M. Hakama, *J. Natl. Cancer. Inst.* **2001**, *93*, 552.
[62] S. W. Lee, P. E. Laibinis, *Biomaterials* **1998**, *19*, 1669.
[63] E. Ostuni, R. G. Chapman, R. E. Holmlin, S. Takayama, G. M. Whitesides, *Langmuir* **2001**, *17*, 5605.
[64] L. A. Ruiz-Taylor, T. L. Martin, F. G. Zaugg, K. Witte, P. Indermuhle, S. Nock, P. Wagner, *PNAS* **2001**, *98*, 852.
[65] M. H. Ravindranath, R. M. H. Ravindranath, D. L. Morton, M. C. Graves, *J. Immunol. Meth.* **1994**, *169*, 257.
[66] S. K. Bhatia, L. C. Shriverlake, K. J. Prior, J. H. Georger, J. M. Calvert, R. Bredehorst, F. S. Ligler, *Anal. Biochem.* **1989**, *178*, 408.
[67] W. Kusnezow, A. Jacob, A. Walijew, F. Diehl, J. D. Hoheisel, *Proteomics* **2003**, *3*, 254.
[68] C. A. Marquette, L. J. Blum, *Biosens. Bioelectron.* **2006**, *21*, 1424.
[69] R. Ekins, P. Edwards, *Clin. Chem.* **1997**, *43*, 1824.
[70] A. D. McNaught, A. Wilkinson, *IUPAC Compendium of Chemical Terminology*, Blackwell Science, Oxford **1997**.
[71] R. P. Buck, E. Lindner, *Pure Appl. Chem.* **1994**, *66*, 2527.
[72] K. Kerman, N. Nagatani, M. Chikae, T. Yuhi, Y. Takamura, E. Tamiya, *Anal. Chem.* **2006**, *78*, 5612.
[73] U. H. Stenman, H. Alfthan, K. Hotakainen, *Clin. Biochem.* **2004**, *37*, 549.
[74] M. J. Eddowes, *Anal. Proc.* **1989**, *26*, 152.
[75] F. Patolsky, A. Lichtenstein, I. Willner, *Nat. Biotechnol.* **2001**, *19*, 253.
[76] L. Alfonta, A. Bardea, O. Khersonsky, E. Katz, I. Willner, *Biosens. Bioelectron.* **2001**, *16*, 675.
[77] X. B. Yu, R. Lv, Z. Q. Ma, Z. H. Liu, Y. H. Hao, Q. Z. Li, D. K. Xu, *Analyst* **2006**, *131*, 745.
[78] K.-S. Ma, H. Zhou, J. Zoval, M. Madou, *Sens. Actuators, B* **2006**, *114*, 58.
[79] S.-J. Park, T. A. Taton, C. A. Mirkin, *Science* **2002**, *295*, 1503.
[80] J. Li, M. Xue, H. Wang, L. Cheng, L. Gao, Z. H. Lu, M. S. Chan, *Analyst* **2003**, *128*, 917.
[81] L. Moreno-Hagelsieb, P. E. Lobert, R. Pampin, D. Bourgeois, J. Remacle, D. Flandre, *Sens. Actuators, B* **2004**, *98*, 269.
[82] F. Patolsky, A. Lichtenstein, I. Willner, *Angew. Chem. Int. Ed.* **2000**, *39*, 940.
[83] A. Bardea, F. Patolsky, A. Dagan, I. Willner, *Chem. Commun.* **1999**, 21.

[84] R. J. Pei, Z. L. Cheng, E. K. Wang, X. R. Yang, *Biosens. Bioelectron.* **2001**, *16*, 355.
[85] H. Chen, J. H. Jiang, Y. Huang, T. Deng, J. S. Li, G. L. Shen, R. Q. Yu, *Sens. Actuators, B* **2006**, *117*, 211.
[86] G. A. Michaud, M. Salcius, F. Zhou, R. Bangham, J. Bonin, H. Guo, M. Snyder, P. F. Predki, B. I. Schweitzer, *Nat. Biotechnol.* **2003**, *21*, 1509.
[87] G. MacBeath, *Nature Genetics* **2002**, *32*, 526.
[88] J. M. Fremy, E. Usleber, *J. AOAC International* **2003**, *86*, 868.
[89] S. A. Soper, K. Brown, A. Ellington, B. Frazier, G. Garcia-Manero, V. Gau, S. I. Gutman, D. F. Hayes, B. Korte, J. L. Landers, D. Larson, F. Ligler, A. Majumdar, M. Mascini, D. Nolte, Z. Rosenzweig, J. Wang, D. Wilson, *Biosens. Bioelectron.* **2006**, *21*, 1932.
[90] O. A. Sadik, H. Xu, E. Gheorghiu, D. Andreescu, C. Balut, M. Gheorghiu, D. Bratu, *Anal. Chem.* **2002**, *74*, 3142.
[91] G. Barbero, A. L. Alexe-Ionescu, I. Lelidis, *J. Appl. Phys.* **2005**, *98*, 113703.
[92] J. E. Garland, C. M. Pettit, D. Roy, *Electrochim. Acta* **2004**, *49*, 2623.
[93] J. Hazi, D. M. Elton, W. A. Czerwinski, J. Schiewe, V. A. Vicente-Beckett, A. M. Bond, *J. Electroanal. Chem.* **1997**, *437*, 1.
[94] C. Berggren, B. Bjarnason, G. Johansson, *Instrum. Sci. Technol.* **1999**, *27*, 131.
[95] H. Kahlert, in *Electroanalytical Methods: Guide to Experiments and Applications* (Ed: F. Scholz), Springer, New York **2002**, pp. 261 – 278.
[96] D. D. Macdonald, *Electrochim. Acta* **2006**, *51*, 1376.
[97] J. R. Macdonald, J. Schoonman, A. P. Lehnen, *J. Electroanal. Chem.* **1982**, *131*, 77.
[98] M. E. Orazem, P. Agarwal, L. H. Garciarubio, *J. Electroanal. Chem.* **1994**, *378*, 51.
[99] R. de Levie, *Electrochim. Acta* **1965**, *10*, 395.
[100] S. H. Liu, *Phys. Rev. Lett.* **1985**, *55*, 529.
[101] T. Pajkossy, *J. Electroanal. Chem.* **1994**, *364*, 111.
[102] Z. Kerner, T. Pajkossy, *Electrochim. Acta* **2000**, *46*, 207.
[103] F. Heer, W. Franks, A. Blau, S. Taschini, C. Ziegler, A. Hierlemann, H. Baltes, *Biosens. Bioelectron.* **2004**, *20*, 358.
[104] J. B. Bates, Y. T. Chu, W. T. Stribling, *Phys. Rev. Lett.* **1988**, *60*, 627.
[105] J. B. Jorcin, M. E. Orazem, N. Pebere, B. Tribollet, *Electrochim. Acta* **2006**, *51*, 1473.
[106] R. J. Stokes, D. F. Evans, *Fundamentals of Interfacial Engineering*, Wiley-VCH, New York **1997**.
[107] M. J. Madou, R. Cubicciotti, *Proc. IEEE* **2003**, *91*, 830.
[108] A. Hassibi, S. Zahedi, R. Navid, R. W. Dutton, T. H. Lee, *J. Appl. Phys.* **2005**, *97*, 084701.
[109] P. R. Nair, M. A. Alam, *Appl. Phys. Lett.* **2006**, *88*, 233120.
[110] D. C. Jiang, J. Tang, B. H. Liu, P. Y. Yang, J. L. Kong, *Anal. Chem.* **2003**, *75*, 4578.
[111] C. Berggren, G. Johansson, *Anal. Chem.* **1997**, *69*, 3651.
[112] G. Shen, N. Tercero, M. A. Gaspar, B. Varughese, K. Shepard, R. Levicky, *J. Am. Chem. Soc.* **2006**, *128*, 8427 – 8433.
[113] T. Komura, T. Yamaguchi, H. Shimatani, R. Okushio, *Electrochim. Acta* **2004**, *49*, 597.
[114] Y. T. Long, C. Z. Li, H. B. Kraatz, J. S. Lee, *Biophys. J.* **2003**, *84*, 3218.
[115] X. H. Li, J. S. Lee, H. B. Kraatz, *Anal. Chem.* **2006**, *78*, 6096.
[116] M. C. Rodriguez, A. N. Kawde, J. Wang, *Chem. Commun.* **2005**, 4267.
[117] H. Cai, T. M.-H. Lee, I. M. Hsing, *Sens. Actuators, B* **2006**, *114*, 433.
[118] S.-J. Ding, B.-W. Chang, C.-C. Wu, M.-F. Lai, H.-C. Chang, *Electrochim. Acta* **2005**, *50*, 3660.
[119] T. Kakiuchi, M. Iida, S. Imabayashi, K. Niki, *Langmuir* **2000**, *16*, 5397.
[120] R. Schweiss, C. Werner, W. Knoll, *J. Electroanal. Chem.* **2003**, *540*, 145.
[121] H. S. White, J. D. Peterson, Q. Z. Cui, K. J. Stevenson, *J. Phys. Chem. B* **1998**, *102*, 2930.
[122] R. Schweiss, D. Pleul, F. Simon, A. Janke, P. B. Welzel, B. Voit, W. Knoll, C. Werner, *J. Phys. Chem. B* **2004**, *108*, 2910.
[123] C. P. Smith, H. S. White, *Langmuir* **1993**, *9*, 1.
[124] W. R. Fawcett, M. Fedurco, Z. Kovacova, *Langmuir* **1994**, *10*, 2403.
[125] Y. Miura, S. Kimura, S. Kobayashi, Y. Imanishi, J. Umemura, *Biopolymers* **2000**, *55*, 391.
[126] I. Burgess, B. Seivewright, R. B. Lennox, *Langmuir* **2006**, *22*, 4420.
[127] R. P. Janek, W. R. Fawcett, A. Ulman, *Langmuir* **1998**, *14*, 3011.
[128] S. O. Kelley, J. K. Barton, N. M. Jackson, L. D. McPherson, A. B. Potter, E. M. Spain, M. J. Allen, M. G. Hill, *Langmuir* **1998**, *14*, 6781.
[129] K. Kitagawa, T. Morita, S. Kimura, *Angew. Chem. Int. Ed.* **2005**, *44*, 6330.
[130] J. Lahann, S. Mitragotri, T. N. Tran, H. Kaido, J. Sundaram, I. S. Choi, S. Hoffer, G. A. Somorjai, R. Langer, *Science* **2003**, *299*, 371.
[131] B. Liu, A. J. Bard, C. Z. Li, H. B. Kraatz, *J. Phys. Chem. B* **2005**, 109, 5193.
[132] F. J. Mearns, E. L. S. Wong, K. Short, D. B. Hibbert, J. J. Gooding, *Electroanalysis* **2006**, *18*, 1971.
[133] A. Gebbert, M. Alvarezicaza, W. Stocklein, R. D. Schmid, *Anal. Chem.* **1992**, *64*, 997.
[134] C. Z. Li, Y. L. Liu, J. H. T. Luong, *Anal. Chem.* **2005**, *77*, 478.
[135] A. Swietlow, M. Skoog, G. Johansson, *Electroanalysis* **1992**, *4*, 921.
[136] J. A. M. Sondag-Huethorst, L. G. J. Fokkink, *Langmuir* **1995**, *11*, 2237.
[137] F. Kremer, A. Schèonhals, *Broadband Dielectric Spectroscopy*, Springer, New York **2003**.
[138] Y. Feldman, I. Ermolina, Y. Hayashi, *IEEE Trans. Diel Electr. Insul.* **2003**, *10*, 728.
[139] K. Youngbok, A. Agarwal, S. R. Sonkusale, *IEEE ISCAS* **2005**, 5906-9.
[140] G. R. Facer, D. A. Notterman, L. L. Sohn, *Appl. Phys. Lett.* **2001**, *78*, 996.
[141] F. Bordi, C. Cametti, R. H. Colby, *J. Phys.: Condens. Matter* **2004**, *16*, R1423.
[142] Y. Hayashi, N. Miura, J. Isobe, N. Shinyashiki, S. Yagihara, *Biophys. J.* **2000**, *79*, 1023.
[143] J. J. Gooding, C. Wasiowych, D. Barnett, D. B. Hibbert, J. N. Barisci, G. G. Wallace, *Biosens. Bioelectron.* **2004**, *20*, 260.
[144] C. M. Li, C. Q. Sun, S. Song, V. E. Choong, G. Maracas, X. J. Zhang, *Front. Biosci.* **2005**, *10*, 180.
[145] P. Ferloni, M. Mastragostino, L. Meneghello, *Electrochim. Acta* **1996**, *41*, 27.
[146] S. Delaney, J. K. Barton, *J. Org. Chem.* **2003**, *68*, 6475.
[147] O. Legrand, D. Cote, U. Bockelmann, *Phys. Rev. E* **2006**, *73*, 31925.
[148] E. L. S. Wong, J. J. Gooding, *Anal. Chem.* **2006**, *78*, 2138.
[149] C. Berggren, B. Bjarnason, G. Johansson, *Biosens. Bioelectron.* **1998**, *13*, 1061.
[150] Z. S. Wu, J. S. Li, T. Deng, M. H. Luo, G. L. Shen, R. Q. Yu, *Anal. Biochemistry* **2005**, *337*, 308.
[151] M. Bart, E. C. A. Stigter, H. R. Stapert, G. J. De Jong, W. P. Van Bennekom, *Biosens. Bioelectron.* **2005**, *21*, 49.
[152] R. D. Johnson, F. H. Arnold, *Biochim. Biophys. Acta* **1995**, *1247*, 293.
[153] P. Bergveld, *Sens. Actuators, B* **2003**, *88*, 1.

[154] V. M. Mirsky, M. Riepl, O. S. Wolfbeis, *Biosens. Bioelectron.* **1997**, *12*, 977.
[155] J. Y. Liu, S. J. Tian, P. E. Nielsen, W. Knoll, *Chem. Commun.* **2005**, 2969.
[156] C. Ouerghi, A. Touhami, N. Jaffrezic-Renault, C. Martelet, H. Ben Ouada, S. Cosnier, *IEEE Sens. J.* **2004**, *4*, 559.
[157] T. L. Lasseter, W. Cai, R. J. Hamers, *Analyst* **2004**, *129*, 3.
[158] H. C. W. Hays, P. A. Millner, M. I. Prodromidis, *Sens. Actuators, B* **2006**, *114*, 1064.
[159] A. Hassibi, T. H. Lee, *IEEE Sens. J.* **2006**, *6*, 1380.
[160] J. C. Love, L. A. Estroff, J. K. Kriebel, R. G. Nuzzo, G. M. Whitesides, *Chem. Rev.* **2005**, *105*, 1103.
[161] D. K. Aswal, S. Lenfant, D. Guerin, J. V. Yakhmi, D. Vuillaume, *Anal. Chim. Acta* **2006**, *568*, 84.
[162] R. Y. Lai, D. S. Seferos, A. J. Heeger, G. C. Bazan, K. W. Plaxco, *Langmuir* **2006**, *22*, 10796.
[163] C. D. Bain, E. B. Troughton, Y. T. Tao, J. Evall, G. M. Whitesides, R. G. Nuzzo, *J. Am. Chem. Soc.* **1989**, *111*, 321.
[164] G. E. Poirier, M. J. Tarlov, H. E. Rushmeier, *Langmuir* **1994**, *10*, 3383.
[165] M. Riepl, V. M. Mirsky, I. Novotny, V. Tvarozek, V. Rehacek, O. S. Wolfbeis, *Anal. Chim. Acta* **1999**, *392*, 77.
[166] E. Boubour, R. B. Lennox, *Langmuir* **2000**, *16*, 4222.
[167] S. Campuzano, M. Pedrero, C. Montemayor, E. Fatas, J. M. Pingarron, *J. Electroanal. Chem.* **2006**, *586*, 112.
[168] E. Boubour, R. B. Lennox, *Langmuir* **2000**, *16*, 7464.
[169] H. Hagenstroem, M. A. Schneeweiss, D. M. Kolb, *Langmuir* **1999**, *15*, 2435.
[170] E. Boubour, R. B. Lennox, *J. Phys. Chem. B* **2000**, *104*, 9004.
[171] E. Pavlovic, A. P. Quist, U. Gelius, L. Nyholm, S. Oscarsson, *Langmuir* **2003**, *19*, 4217.
[172] L. M. Tender, R. L. Worley, H. Y. Fan, G. P. Lopez, *Langmuir* **1996**, *12*, 5515.
[173] J. Wang, M. Jiang, A. M. Kawde, R. Polsky, *Langmuir* **2000**, *16*, 9687.
[174] R. Y. Lai, S. H. Lee, H. T. Soh, K. W. Plaxco, A. J. Heeger, *Langmuir* **2006**, *22*, 1932.
[175] M. Dijksma, B. Kamp, J. C. Hoogvliet, W. P. van Bennekom, *Langmuir* **2000**, *16*, 3852.
[176] M. Dijksma, B. A. Boukamp, B. Kamp, W. P. van Bennekom, *Langmuir* **2002**, *18*, 3105.
[177] J. Rickert, W. Gopel, W. Beck, G. Jung, P. Heiduschka, *Biosens. Bioelectron.* **1996**, *11*, 757.
[178] R. A. Potyrailo, R. C. Conrad, A. D. Ellington, G. M. Hieftje, *Anal. Chem.* **1998**, *70*, 3419.
[179] S. Klussmann, *The Aptamer Handbook: Functional Oligonucleotides and their Applications*, Wiley-VCH, Weinheim **2006**.
[180] A. D. Ellington, J. W. Szostak, *Nature* **1990**, *346*, 818.
[181] C. Tuerk, L. Gold, *Science* **1990**, *249*, 505.
[182] S. Tombelli, A. Minunni, A. Mascini, *Biosens. Bioelectron.* **2005**, *20*, 2424.
[183] W. H. Robinson, C. DiGennaro, W. Hueber, B. B. Haab, M. Kamachi, E. J. Dean, S. Fournel, D. Fong, M. C. Genovese, H. E. N. de Vegvar, K. Skriner, D. L. Hirschberg, R. I. Morris, S. Muller, G. J. Pruijn, W. J. van Venrooij, J. S. Smolen, P. O. Brown, L. Steinman, P. J. Utz, *Nat. Med.* **2002**, *8*, 295.
[184] A. L. Newman, K. W. Hunter, W. D. Stanbro, *Chemical Sensors: 2nd International Meeting, Proc.* **1986**, 596–598.
[185] R. F. Taylor, I. G. Marenchic, R. H. Spencer, *Anal. Chim. Acta* **1991**, *249*, 67.
[186] H. Maupas, C. Saby, C. Martelet, N. JaffrezicRenault, A. P. Soldatkin, M. H. Charles, T. Delair, B. Mandrand, *J. Electroanal. Chem.* **1996**, *406*, 53.
[187] H. Maupas, A. P. Soldatkin, C. Martelet, N. Jaffrezic-Renault, B. Mandrand, *J. Electroanal. Chem.* **1997**, *421*, 165.
[188] C. Berggren, P. Stalhandske, J. Brundell, G. Johansson, *Electroanalysis* **1999**, *11*, 156.
[189] M. Hedstrom, I. Y. Galaev, B. Mattiasson, *Biosens. Bioelectron.* **2005**, *21*, 41.
[190] W. Limbut, P. Kanatharana, B. Mattiasson, P. Asawatreratanakul, P. Thavarungkul, *Biosens. Bioelectron.* **2006**, *22*, 233.
[191] Y. M. Zhou, S. Q. Hu, Z. X. Cao, G. L. Shen, R. Q. Yu, *Anal. Lett.* **2002**, *35*, 1919.
[192] D. C. Jiang, J. Tang, B. H. Liu, P. Y. Yang, X. R. Shen, J. L. Kong, *Biosens. Bioelectron.* **2003**, *18*, 1183.
[193] S. Zhang, J. J. Ding, Y. Liu, J. L. Kong, O. Hofstetter, *Anal. Chem.* **2006**, *78*, 7592.
[194] S. Q. Hu, Z. M. Xie, C. X. Lei, G. L. Shen, R. Q. Yu, *Sens. Actuators, B* **2005**, *106*, 641.
[195] K. Wang, D. C. Jiang, J. L. Kong, S. Zhang, B. H. Liu, T. P. Lu, *Anal. Lett.* **2003**, *36*, 2571.
[196] M. Dijksma, B. Kamp, J. C. Hoogvliet, W. P. van Bennekom, *Anal. Chem.* **2001**, *73*, 901.
[197] Y. T. Long, C. Z. Li, T. C. Sutherland, H. B. Kraatz, J. S. Lee, *Anal. Chem.* **2004**, *76*, 4059.
[198] X. H. Li, Y. L. Zhou, T. C. Sutherland, B. Baker, J. S. Lee, H. B. Kraatz, *Anal. Chem.* **2005**, *77*, 5766.
[199] C. Z. Li, Y. T. Tong, J. S. Lee, H. B. Kraatz, *Chem. Commun.* **2004**, 574.
[200] Y. Akagi, M. Makimura, Y. Yokoyama, M. Fukazawa, S. Fujiki, M. Kadosaki, K. Tanino, *Electrochim. Acta* **2006**, *51*, 6367.
[201] D. K. Xu, D. W. Xu, X. B. Yu, Z. H. Liu, W. He, Z. Q. Ma, *Anal. Chem.* **2005**, *77*, 5107.
[202] S. Ameur, C. Martelet, N. Jaffrezic-Renault, J. M. Chovelon, *Appl. Biochem. Biotechnol.* **2000**, *89*, 161.
[203] J. C. Pyun, S. D. Kim, J. W. Chung, *Anal. Biochem.* **2005**, *347*, 227.
[204] S. Cosnier, *Electroanalysis* **2005**, *17*, 1701.
[205] G. Lillie, P. Payne, P. Vadgama, *Sens. Actuators, B* **2001**, *78*, 249.
[206] F. Darain, D. S. Park, J. S. Park, Y. B. Shim, *Biosens. Bioelectron.* **2004**, *19*, 1245.
[207] C. Tlili, H. Korri-Youssoufi, L. Ponsonnet, C. Martelet, N. Jaffrezic-Renault, 2005 *Conf. Solid-State Sensors, Actuators Microsys.* **2005**, 1600.
[208] H. Z. Huang, Z. G. Liu, X. R. Yang, *Anal. Biochem.* **2006**, *356*, 208.
[209] Y. Z. Fu, R. Yuan, L. Xu, Y. Q. Chai, Y. Liu, D. P. Tang, Y. Zhang, *J. Biochem. Biophys. Meth.* **2005**, *62*, 163.
[210] M. S. DeSilva, Y. Zhang, P. J. Hesketh, G. J. Maclay, S. M. Gendel, J. R. Stetter, *Biosens. Bioelectron.* **1995**, *10*, 675.
[211] S. C. Pak, W. Penrose, P. J. Hesketh, *Biosens. Bioelectron.* **2001**, *16*, 371.
[212] A. V. Mamishev, K. Sundara-Rajan, F. Yang, Y. Q. Du, M. Zahn, *Proc. IEEE* **2004**, *92*, 808.
[213] W. Laureyn, D. Nelis, P. Van Gerwen, K. Baert, L. Hermans, R. Magnee, J. J. Pireaux, G. Maes, *Sens. Actuators, B* **2000**, *68*, 360.
[214] T. C. Hang, A. Guiseppi-Elie, *Biosens. Bioelectron.* **2004**, *19*, 1537.
[215] C. Guiducci, C. Stagni, G. Zuccheri, A. Bogliolo, L. Benini, B. Samori, B. Ricco, *Biosens. Bioelectron.* **2004**, *19*, 781.
[216] C. Stagni, C. Guiducci, L. Benini, B. Ricco, S. Carrara, B. Samori, C. Paulus, M. Schienle, M. Augustyniak, R. Thewes, *IEEE JSSC* **2006**, *41*, 2956.
[217] C. Guiducci, C. Stagni, A. Fischetti, U. Mastromatteo, L. Benini, B. Ricco, *IEEE Sens. J.* **2006**, *6*, 1084.
[218] A. Hassibi, T. H. Lee, *2005 IEEE ISSCC* **2005**, *1*, 564.
[219] S. D. Senturia, *IEEE Trans. Ultrason. Ferr. Freq. Contr.* **2004**, *51*, 127.
[220] P. T. Kissinger, *Biosens. Bioelectron.* **2005**, *20*, 2512.

